IMPERIAL COLLEGE LONDON

Department of Earth Science and Engineering

Centre for Petroleum Studies

Liquids-Rich Shale Evaluation: Modelling and Optimization of Hydraulically Fractured Liquids-Rich Shale Wells

Formatted: Centered

By

Marco Cunha

A report submitted in partial fulfilment of the requirements
for the MSc and/or the DIC

September 2013

DECLARATION OF OWN WORK

I declare that this thesis:

Liquids Rich Shale Evaluation

-is entirely my own work and that where any material could be construed as the work of others, it is fully cited and referenced, and/or with appropriate acknowledgement given.

Signature:.....

Name of student: **Marco Cunha**

Name of supervisor: **Alain Gringarten, Genevieve Young**

Abstract

Advances in hydraulic fracture stimulation of shale gas reservoirs have unlocked unconventional natural gas reserves worldwide. In recent years the industry has become increasingly aware of the benefits that can be derived from the development of liquids-rich shale reservoirs. Due to the increased revenue associated with liquids production, these types of shales have become attractive, particularly in a market which so heavily favours liquids.

This work focuses on the modelling and optimization of liquids-rich shale reservoirs, and aims to identify optimal strategies for production. A representative model utilizing symmetry elements is built with properties based on the liquids-rich region of the Eagle Ford shale in Texas. Methods of grid arrangement are compared and the impact of grid resolution on planar fracture models is investigated. It is shown that relatively coarse grids are able to yield representative results and be used effectively in production strategy studies involving large numbers of runs. The impact of bottom-hole pressure on present value is investigated for various reservoir pressures, and optimum operating bottom-hole pressures are proposed. Sensitivities are then conducted on various reservoir parameters to assess their impact on production optimization and on present value.

Two lean gas condensate fluids are considered as in-situ fluids with condensate gas ratios (CGRs) of 30 and 75 Stb/MMscf. The effect of each of these fluids on production performance is evaluated from a revenue perspective, and production optimization strategies are proposed. Some discussion into near-critical fluid modelling in ultra-low permeability reservoirs is also included, using a fluid with a CGR of 150 Stb/MMscf.

Consideration is given to the various phenomena encountered in liquids-rich shales that cause the behaviour of these systems to deviate strongly from conventional behaviour. Recommendations for the incorporation of these effects into reservoir models are given, and suggestions for future work are proposed.

Comment [ACG1]: what are these?

Acknowledgements

Firstly I would like to thank BG Group for giving me the opportunity to conduct my thesis with some excellent people, who I have learned much from in ten weeks. In particular I would like to thank Genevieve Young, Alistair Green and Nick Curum for advising me through the entire process, Tim Whittle and Alex Gabb for providing excellent feedback on my written work, Neal Morgan and Candice Ogiste for their help with the petrophysical aspects of the Eagle Ford shale, Paolo Giacon for his input into completion metrics, Marco Misenta for his help with CMG and near-critical modelling and Curtis Whitson for his excellent talk at BG Group from which I learned a great deal.

I would also like to thank my professors at Imperial College, in particular Alain Gringarten for being my academic supervisor and my course mates at Imperial and fellow interns for providing help and support.

I am also grateful to Andrew Scott and Conoco Philips for providing sponsorship for my MSc program, I could not have done it without this and I would have missed out a great deal.

Contents

Figures

Tables

Imperial College London

Liquids-Rich Shale Evaluation: Modelling and Optimization of Hydraulically Fractured Liquids-Rich Shale Wells

M. Cunha, Imperial College London, BG Group

Introduction

Comment [ACG2]: this must be preceded by the abstract. It seems the you are using this trick along with references to appendices to stay within the 16 page limt!

Recent publications on the topic of liquids-rich shale production have highlighted the detrimental effect that liquid dropout in the reservoir can have on production (D. Ilk, 2012). Some studies have suggested that there is possibility of an optimal bottom hole flowing pressure that is significantly higher than would be for conventional systems, and so are in favour of an operating strategy where the well is choked back (C. H. Whitson, 2012). This is largely due to the extremely low permeabilities and pore sizes in shale, as the relative permeabilities of the liquid phase dictate that generally any liquid dropped out within the reservoir is effectively immobile, and rather than contributing to production will only serve as a barrier to gas flow (D. Ilk, 2012). Identifying this optimal point is of importance if the revenue from these systems is to be maximized, as the cost of identifying a false optimum point could be significant. A good knowledge of the in-situ conditions and parameters of the particular system such as the in-situ fluid composition, matrix properties, reservoir pressure, temperature, and completions metrics is vital to the successful design of a representative model.

Unfortunately the nature of shale makes it very difficult to accurately determine many of these values. In-situ fluid composition is particularly difficult to obtain, not only due to the liquid dropout effect discussed but also due to other more complex production mechanisms such as desorption. It is therefore difficult to define the phase envelope and saturation pressure with accuracy unless the fluid samples are taken at very low drawdown, and very early on in the life of the well in order to minimize these effects (C. H. Whitson, 2012). Matrix properties are also difficult to measure. Because the permeabilities are so low, they prohibit the use of conventional permeability measurement techniques and instead are measured using crushed samples. While this removes sample damage from the coring process, any natural fractures existing in-situ will also be destroyed.

Microseismic monitoring can go some way towards describing the propagation of hydraulic fractures during the fracturing process, however there is no direct method to measure the conductivity of these fractures and therefore any estimation of the effective half-length and conductivity relies on empirical evidence and knowledge of the performance of historic hydraulic stimulations in the formation. There is a great deal of uncertainty involved in describing these types of systems and all of these uncertainties go towards the difficulty of building truly representative models.

Pressure transient analysis has the potential to reduce uncertainties in fracture and reservoir properties and the impact of reservoir fluid properties. However, it is not currently common practice to install bottom-hole pressure gauges on shale wells and hence the use of pressure transient analysis has not been considered in this study. A recommendation for future work exploring the utilization of pressure transient analysis to characterize unconventional reservoirs has been included in the discussion.

This study uses the liquids-rich region of the Eagle Ford shale play in South Texas as a base case from which representative parameters are taken. The aim is to address the modelling of liquids rich systems from a well-life optimization perspective, as well as investigate optimal production strategies that may help to increase revenue. The gridding of 3D liquids rich shale models is investigated, and optimal gridding methods are determined for compositional models. The effect of production strategy on revenue is also analysed, and the impacts of uncertainties and unconventional phenomena are discussed.

Literature Review and Base Case Parameter Selection

The Eagle Ford formation overlays the Buda limestone, and has traditionally been thought of as the source rock for the Austin Chalk, which directly overlays it. Figure 1 (C&C Reservoirs, 2011) shows how the Eagle Ford is positioned in Texas, and how the different fluid regions are arranged.

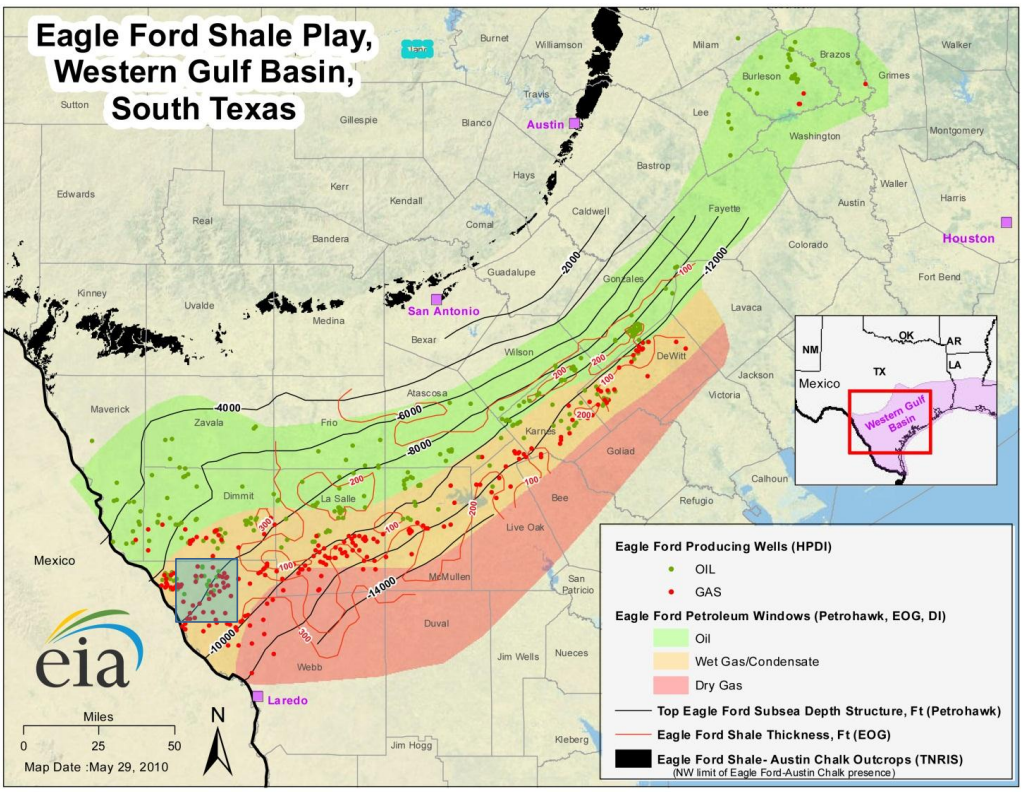

Figure 1: Map of Eagle Ford overlaid on map of Texas with fluid, thickness, and depth information (Energy Institute)

The region of interest to this study is shown in yellow in the above picture. The region of North-west Webb County Texas close to the Mexico - USA border is chosen as a primary basis for design (shown in the blue square). The thickness in this area is consistent with an average of 200 ft and there a good selection of well data available mainly comprising of core data, with an even overlap of 'oil' and 'gas' wells. The depth varies from 6000 to 12000 ft in some parts of the liquids-rich region. A thickness of **200 ft** and a depth of **10000 ft** is chosen for the model, it should be noted that the reference depth does not have any direct effect on the simulation, and is only included for consistency of data.

Due to the gas maturation process, the Eagle Ford is significantly over pressured (R. Shelley, 2012). A base case initial pressure of **7000 psia** is chosen along with an initial temperature of **250 °F.** These values are typical of what is observed in well data (C&C Reservoirs, 2011) and consistent with what previous authors have used in their studies (D. Ilk, 2012). Rock compressibility is assumed to be constant for the model. It has been suggested that due to the high concentration of smectite in the shale, the Eagle Ford would be expected to have a relatively high compressibility (A. S. Chaudhary, 2011). A compressibility of **25 μ psi^{-1}** is chosen for the base case.

The well is assumed to be one of many in a repeating well pattern, and fractured in identical stages of equal length along the wellbore. This assumption allows a single fracture – or symmetry element of a fracture – to be modelled as a sub-model rather than an entire well model. The production rates from the sub-model are then scaled up to the entire well.

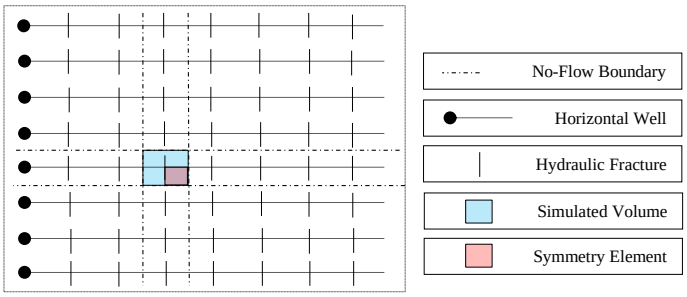

Figure 2: Areal view of a repeating well pattern with simulated region highlighted

Figure 2 shows a schematic aerial view of the repeating well pattern. Considering a single fracture rather than an entire well reduces the simulation time and allows for a much higher level of refinement to be applied within reasonable simulation times. As can be seen, there are no-flow boundaries both between laterals and between planar fractures. As a result, it is important to set the spacing of both lateral wells and of perforation clusters to realistic values in order to fix the geometry of the model. A typical well spacing of **8 wells per square mile** is assumed, along with **12 fracture stages** of **4 perforation clusters** each (D. Ilk, 2012), (C&C Reservoirs, 2011), (Schlumberger, 2009). Equal spacing is also assumed. The size of the simulation grid is therefore constrained to a size of **660 x 105 x 200 ft**. (lateral spacing x fracture spacing x formation thickness). The horizontal well bore length is fixed at **5000 ft**. in line with the **8 well per 640 ac** spacing. A wellbore diameter of **5.5"** is chosen as this is consistent with data on existing Eagle Ford completions (C&C Reservoirs, 2011).

Analysing micro seismic images from hydraulically fractured completions in the Eagle Ford, it is seen that microseismic events occur well into both the Austin Chalk and the Buda limestone above and below the Eagle Ford Shale (R. Shelley, 2012). Microseismic events are frequently recorded up to 300 ft from the wellbore in the horizontal direction. Although these events are observed, it must be noted that they do not translate to infinite conductivity planar fracture geometry. With this in mind, a fracture horizontal half-length of **75 ft**. in the horizontal and **50 ft**. in the vertical is chosen with a hydraulic fracture conductivity of **1 mD.ft.** This was validated by internal consultation[1].

The porosity of the Eagle Ford Shale is relatively well known and measurement techniques are reasonably accurate. A connected gas filled porosity of **0.09** with an initial water saturation of **0.4** is chosen in line with what previous authors have used as well as data from selected wells (A. Orangi, 2011). The permeability on the other hand is a large source of error in the model. Measurements of matrix permeability taken from core samples using pressure decay tests can range anywhere from 0 to over 10000 nD. There is also the complicating factor of possible conductive natural fractures in the matrix, a phenomenon that is not fully understood in the Eagle Ford. As a result of this and in the interests of keeping the model general, an *overall* permeability of **320 nD** in the horizontal and **32 nD** in the vertical direction was assumed[2]. For the purposes of this work it is assumed that any conductive natural fractures in the system were originally sealed and have been opened up as a result of hydraulic treatment. There is therefore no dual permeability behaviour observed in the matrix, and any fracture system is accounted for in the planar fracture. There is also no accommodation for stress or pressure dependant permeability in the base case model; this was a conscious decision made in order to isolate the effects of liquid dropout on production performance.

It is not thought that there is any significant difference in relative permeability or wettability behaviour between shale and other ultra-tight rock types due to the rock itself (C. H. Whitson, 2012). There are however phenomena observed in shale that cannot be explained using conventional approaches. Pores at a nanometre scale could theoretically act as molecular sieves, preventing larger molecules from being conducted through the matrix inducing component separation (D. Devegowda, 2012). Due to the presence of kerogen in the matrix, adsorption effects are also at work, preferentially retaining some molecules within the kerogen pores. These effects and others are discussed in more detail in the discussion. A well life of **30 years** is set with an expected recovery factor of **25%**. Although there is not enough production data currently to confirm these values in the Eagle Ford, they are typical of other authors' predictions (Swindell, 2012) (C&C Reservoirs, 2011) and should be similar to future Eagle Ford production patterns. Relative permeability is highly important to the performance of a liquid rich shale system as it determines the effect that the presence of condensate drop-out in the matrix will have on the flow of gas, and also whether the associated condensate will flow at all. Due to the large amount of time that it would take to run three phase relative permeability experiments on shale – as well as the errors that would be involved – there is very little data available on the relative permeability of shale. The relative permeability data used for the base case of this study was estimated from that which has been used in previous studies (A. Orangi, 2011), the relative permeability in the fracture cells was assumed to be linear[2]. The solubility of all components in the aqueous phase was assumed to be zero.

[1] Personal communication, P. Giacon, Principal Consultant in Production Technology, BG Group
[2] Personal communication, G. Young, Group Technical Authority on Unconventionals, BG Group

Fluid PVT

This study uses compositional fluid data from C. H. Whitson, (2012). The two fluids considered have condensate gas ratios (CGRs) of 30 and 75 Stb/MMScf. According to the study, these fluids are typical of what would be found in-situ in a liquid-rich shale prospect, even though these compositions may not actually be produced at surface due to liquid drop-out. The phase diagrams can be found in the appendices Figures C-1 to C-3. The compositions of the fluids used are also given graphically in Figure C-4. The Peng-Robinson Equation of state was used. The composition and component properties can be found in the appendices Tables C-1 and C-2. The viscosity model used was the Pedersen Corresponding States Principle (CSP). All simulations are run fully compositional and implicitly.

Layering

The possibility of incorporating layering into the model was investigated. It was thought that there may be some correlation between depth and porosity or depth and permeability. In order to verify this, these properties were both plotted against the property normalized formation depth. The normalized formation depth is taken as the fraction through the formation and can be calculated as:

$$NFD = {k - k_{top}}/{k_{base} - k_{top}}$$

Where:

k_{top} = measurement depth
k_{top} = depth at the top of the formation
k_{base} = depth at the base of the formation

Using this measurement of depth makes it easier to view any potential patterns in the formation, and facilitates the identification of laterally continuous trends.

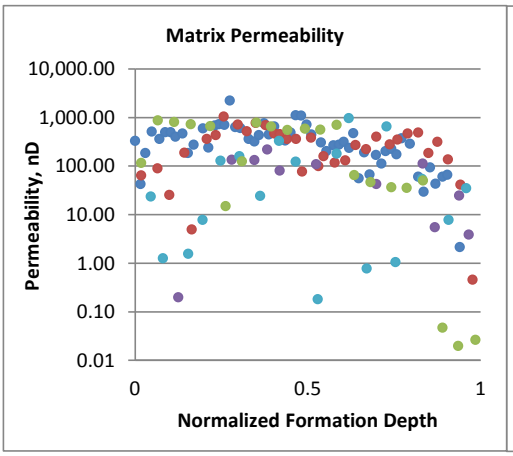

Figure 3: Matrix permeability vs. depth for well in the liquids-rich region of the Eagle Ford shale

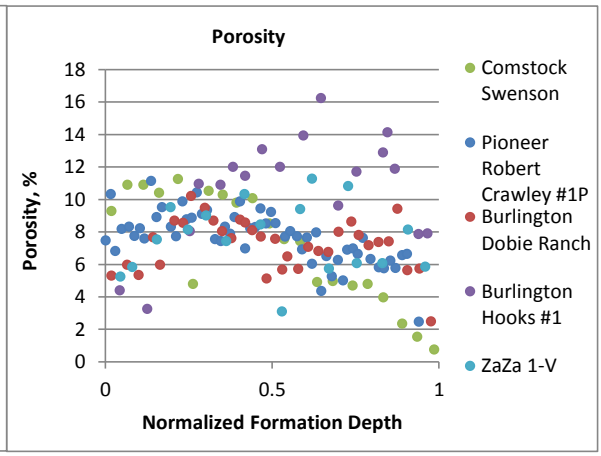

Figure 4: Porosity vs. depth for wells in the liquids-rich region of the Eagle Ford shale

As shown by Figures 3 and 4, there is no laterally generalizable correlation observed in the Eagle Ford shale, either for permeability or porosity. There is a slight tendency towards lower permeabilities and porosities with increasing depth, however the correlations are very weak (R^2 correlation values between 0 and 0.7) and - in the interests of keeping the model general – they were not included. This decision was also validated by consultation[3]. Figure F-1 in the appendices illustrates the pressure and saturation distributions across the model, operated at a bottom-hole pressure of 1400 psi.

[3] Personal communication, Candice Ogiste, Petrophysicist, BG Group

Gridding

A planar fracture model was chosen as the preferred modelling strategy for this study. Planar fracture grids have been used with success in numerous previous studies (A. Orangi, 2011; A. S. Chaudhary, 2011) to name two. The geometry of this model is shown in the schematic of Figure E-1 in the appendices. In order to build a realistic yet practical model, it was necessary to select a gridding approach that minimized simulation time, whilst honouring the true behaviour of the model. After some preliminary runs, it was concluded that a uniform gridding approach would be prohibitively expensive in terms of simulation time. It was decided to use a logarithmically refined grid. Logarithmic refinement allows the geometry of the fracture to be accurately captured, whilst minimizing the number of grid cells in the model, and has also been used with success in a number of previous studies (Rubin, 2010; A. S. Chaudhary, 2011). The grid is comprised of two types of cells: matrix cells and fracture cells. The matrix cells are assigned the bulk properties of the formation. The fracture cells however have a permeability that is calculated based on the conductivity of the fracture. The grid is fine close to the fracture face and coarse far from the fracture face which allows for the high pressure and saturation gradients to be captured more accurately.
The grid is then constructed subject to the following constraints.

- No cell can be any more than twice the size of its direct neighbours (numerical stability).
- The refinement factor is constant in each direction.
- The grid must be constructed using the minimum number of cells possible subject to the above rules.

The refinement factor is the ratio of the dimensions of a cell to its neighbouring cells. For example, in a grid with a refinement factor of 0.5 (the minimum allowed by the rules above), cells would halve in size towards the fracture. If the above rules are followed, the fundamental grid construction is based on the chosen dimensions of the perforation cell and the grid is unique for a given perforation block size. When assigning the permeability of the individual fracture cells, the following equation is used. All fracture cells are modelled as being isotropic.

$$C_f = k_f W_f$$

The permeability calculated is assigned to all of the fracture cells that are within the half length of the fracture. For cells that straddle the half length - which occurs in every model due to the logarithmic nature of the grid - an arithmetic average weighted by the portion of cell within the fracture is found, both for the horizontal direction and for the vertical edge cells. The average of these two permeabilities is then found, and applied to the four corners of the fracture as shown in Figure 5.

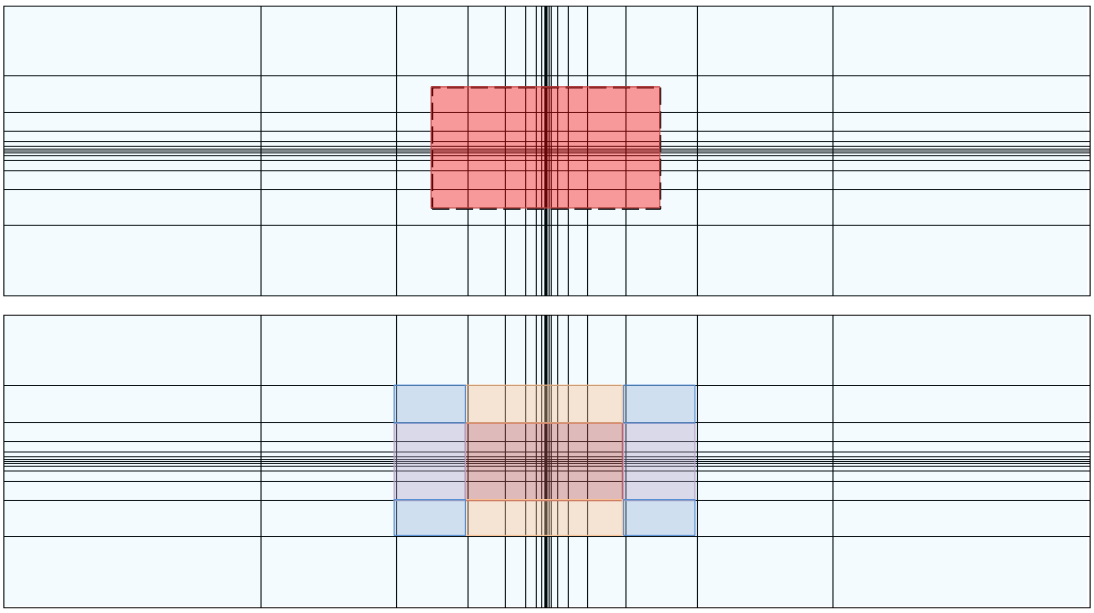

Figure 5: Permeability approximations in fracture edge cells

In order to verify the applicability of this technique, a second grid was built. In this grid, cells are logarithmically refined not only towards the fracture face (LR-FF) but also towards the tips of the fractures (LR-FF-FT). This approach means that the fracture edges lie exactly at cell edges and there is no need to assign any cells average values of permeability as shown in Figure 6. A comparison of the two gridding techniques is shown below in Figure 7. A bottom-hole pressure of 600 psi was used with a CGR 75[4] in situ fluid. The well block was 0.5 x 0.5 x 0.5 ft for both grids.

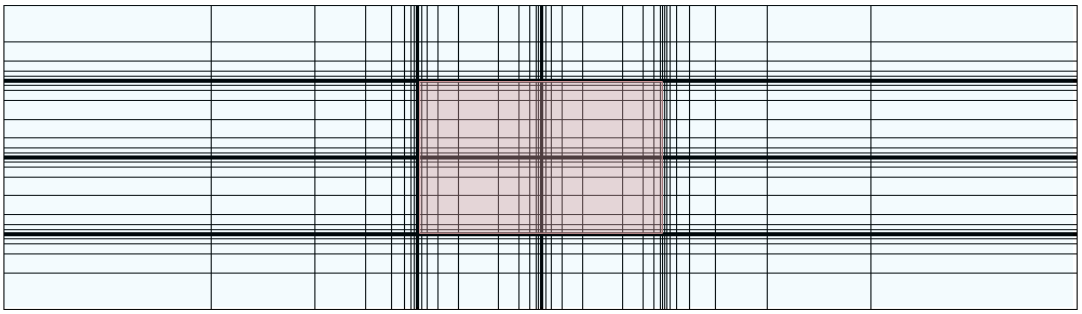

Figure 6: Logarithmic refinement to fracture face and fracture tip (LR-FF-FT)

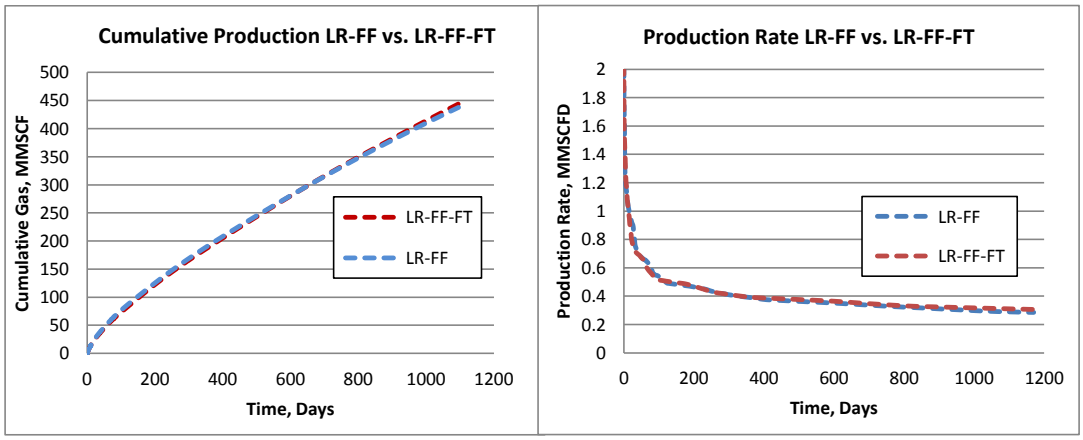

Figure 7: Cumulative gas and rate data for LR-FF and LR-FF-FT type gridding simulation

Figure 7 demonstrates that the LR-FF simulation with edge cell permeability estimation produces nearly the same result as the far more computationally expensive LR-FF-FT method. For this reason the LR-FF method is chosen as the gridding technique for this study.

Liquids-rich shale is unique in that although it has many parallels to conventional gas condensate systems with respect to PVT; it has the complicating factor of ultra-low permeability. This means that the pressure profile near the well can be extremely steep, and therefore the region in which severe liquid dropout occurs is very small. A consequence of this is that to simulate the liquid dropout meaningfully, cell sizes must be small enough in the near wellbore region to reflect the pressure profile in the reservoir. This refinement is mainly relevant in the i-direction – towards the fracture face.

In order to attain a greater level of refinement with the same computational power, a further symmetry element was utilised by splitting the existing model into four. This allowed a higher level of refinement in both i and j directions, so better capturing the liquid dropout. The rules described for grid construction are the same, the only difference being that the grid refinement factor in the i-direction is not minimised to 0.5 but varied to more accurately capture the effects of dropout on production.

[4] CGR 30 and CGR 75 denote the condensate gas ratio in units of Stb/MMScf. This convention is adopted from here on in the study

Verification of Representative Model

Once the properties of the base case model were decided, their validity was verified by comparing the results of a simulation run with field results. Figure 8 shows the simulation results for the first 5 years plotted on the same graph as publically available production data from a well drilled in the Webb County area of the Eagle Ford condensate region. Quarter fracture grid production data has been scaled up to reflect full well rates. Since installing bottom-hole pressure gauges on liquid rich shales is rare[5] a history match was not possible in this study. The early time production deviates from reality, since no restriction has been applied to the maximum rate.

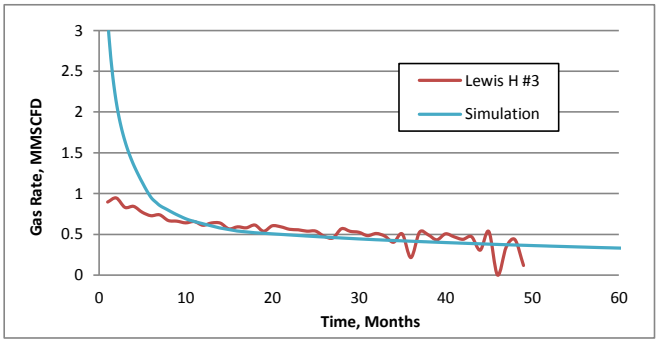

Figure 8: Field decline curves compared with base case simulation

The simulation results appear to be within range of this publicly available production data. Figure B-1 in the appendices shows the estimated ultimate recovery of multiple Eagle Ford wells with the ranges of recovery for the base case model highlighted in comparison. These confirmations, along with the reliable sources of data used in choosing model parameters were taken as sufficient evidence that the model is representative of an Eagle Ford well.

Grid Resolution

In order to reduce the run time for the model, simulations were run using fewer grid blocks than in the reference model. The logarithmic grid refinement technique was still used, and the dimensions can be found in the appendices, in Table . By analysing Figures 9 and 10 it can be seen that simulations run with 14 cells, 10 cells, and 8 cells all predict very similar results for the gas production and show equivalent trends for the condensate gas ratio of the well stream. These simulations were run with the CGR 75 fluid. Little difference was observed when the resolution was changed. An 8-cell model was able to run using a fully implicit compositional model in under 30 minutes. This speed is satisfactory for the studies conducted in this report, and an 8-Cell refinement scheme is able to resolve to a fracture width of 0.25 ft and therefore capture liquid dropout effects well.

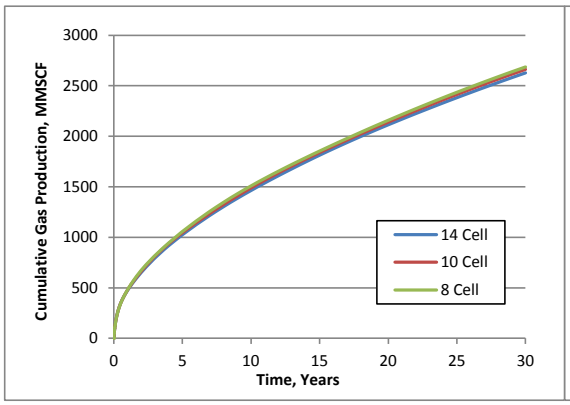

Figure 9: Cumulative simulated gas production for i-direction refinements to 14, 10, and 8 Cells

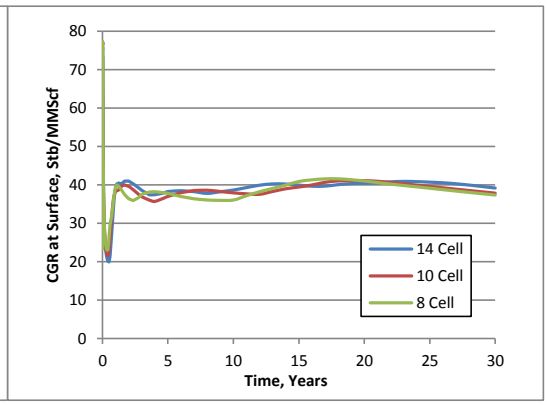

Figure 10: CGR variation with time for i-direction refinements to 14, 10, and 8 Cells

[5] Internal presentation, C. Whitson

Present Value Sensitivity to Bottom-hole flowing Pressure

Figure 11 and Figure 12 display the cumulative oil and gas production over a 30 year period respectively for both the CGR 75 and CGR 30 fluids. Figure 13 shows how the calculated cumulative present value (PV) after 30 years varies for different constant bottom hole flowing pressures for an in situ fluid CGR 75. The PV calculations assume an oil price of 100 USD/Bbl, a gas price of 3 USD/Mscf and a discount rate of 10%. The coloured lines are termed the BHP optimization curves. The dashed grey line indicates the approximate locus of the optimum points for varying reservoir pressures.

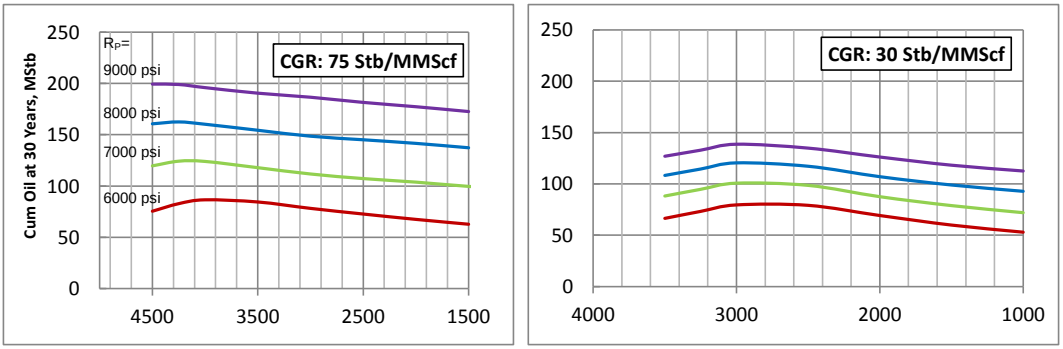

Figure 11: Total predicted 30 year oil production for varying reservoir pressures – CGR 75 and CGR 30 respectively

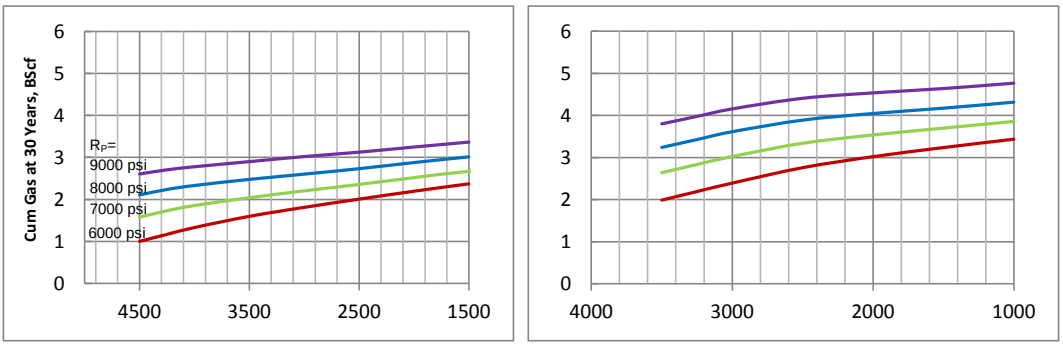

Figure 12: Total predicted 30 year gas production for varying reservoir pressures – CGR 75 and CGR 30 respectively

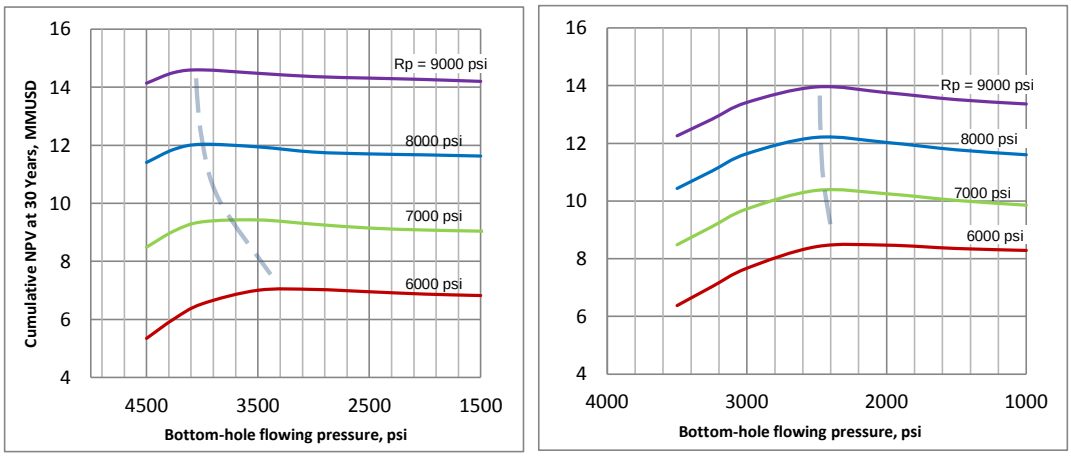

Figure 13: Cumulative NPV at 30 years under varying bottom-hole flowing pressures - CGR 75 and CGR 30 respectively

Typically more gas production is observed with decreasing bottom-hole pressure; however, oil production tends to decrease below a certain bottom-hole pressure and displays a clear optimum point. The locus of the optimum points has been translated onto Figure 14. C. H. Whitson observes (2012) that whilst the optimum drawdown may be the saturation pressure during early times of 100-170 days, it is unlikely that keeping the bottom-hole pressure at the saturation pressure would be optimal in the long term. Figure 14 verifies this claim, but shows that rather than an initial low drawdown followed by maximum drawdown, there is an optimum point for constant BHP that tends to sit just below dew point pressure. This optimum point moves towards lower pressures and becomes less defined at lower initial reservoir pressures. The values presented constitute the present worth of the hydrocarbon stream, and do not include estimates of operational or initial costs. Because of this, it can be reasoned that the increased revenue from operating at optimum point would have a significant impact on the profit margins of the development

Comment [ACG3]: very unclear from Fig. 14. Explain.

.

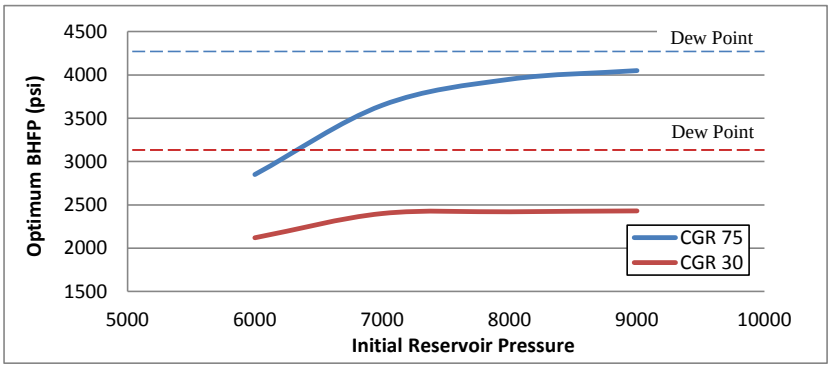

Figure 14: Optimum bottom-hole pressure - CGR 75 and CGR 30 with varying initial reservoir pressure

It is possible that the optimum point predicted may not be evident during production. One operational technique would be to initially flow the well at a bottom-hole pressure that is above the believed optimum point, and gradually reduce the bottom hole flowing pressure whilst monitoring the production to define the optimum operating point. However, since high drawdowns can lead to a build-up of immovable liquid, the observed optimum point may be below the true optimum, and therefore this method could lead to irreversible damage (excess liquid dropout) to the reservoir. It is therefore recommended that this method be followed with caution, in conjunction with the continual revision of a predictive model.

Figure 15 shows revenue from the first 5 years of production of a CGR 75 fluid from the base case model with an initial pressure of 9000 psi and bottom-hole pressures of 3500 psi and 4000 psi. Initially, it seems that producing at 3500 psi may yield the highest overall recovery. However at approximately 1 year into production, the detrimental effects of liquid dropout overtake the effects of higher gas production and the rate of revenue begins to decline with respect to the 4000 psi case. After 2 years it is more economical to produce at 4000 psi and this trend continues for the remainder of the well life.

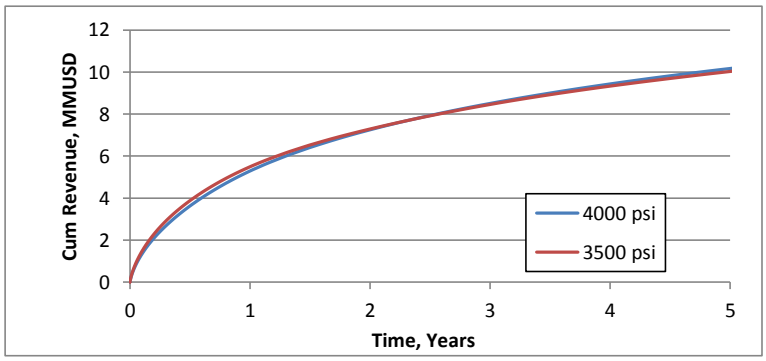

Figure 15: Cumulative PV for the first 5 years with BHPs of 3500 psi and 4000 psi - reservoir pressure is 9000 psi.

Impact of Matrix Permeability on the BHP Optimization Curve

The total permeability of the matrix is an uncertain parameter in the modelling of shale reservoirs. In reality heterogeneity would cause permeability to vary widely, for the purposes of this study, the shale is assumed to have a constant permeability that functions as an average of the true permeability of the formation. Figure 16 shows the impact of varying average matrix permeabilities on the present value curve for varying bottom-hole pressures. Base case permeability is 320 nD.

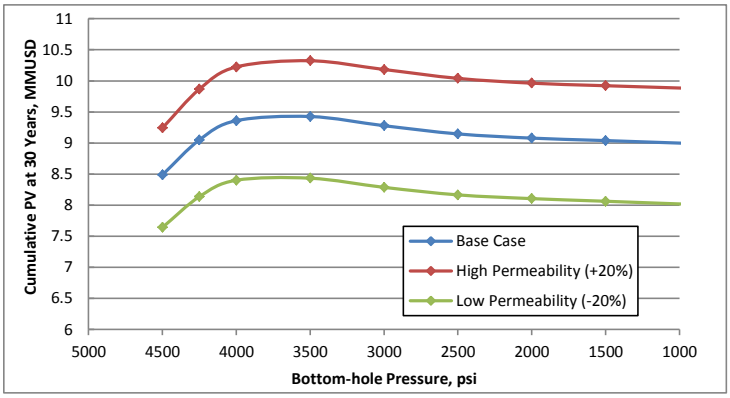

Figure 16: Impact of matrix permeability on BHP optimization curve

The optimum point is still present under varying matrix permeabilities and its value remains unaffected. There is a clear relationship between the matrix permeability and the total present value of the well stream.

Impact of Matrix Porosity on the BHP Optimization Curve

Porosity is less uncertain that permeability in these types of reservoirs. It is however intimately linked with hydrocarbons in place, and therefore strongly related to the total present value of the well stream. Figure 17 shows the impact of varying porosity on the present value curve for varying bottom-hole pressures. Base case porosity is 0.09.

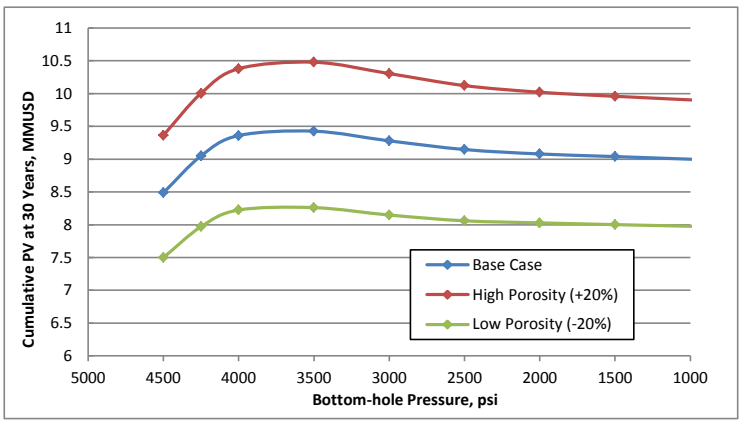

Figure 17: Impact of matrix porosity on BHP optimization curve

The porosity influences the present value of the well stream in a similar manner to the permeability. The curve is shifted towards higher or lower total present values, but the optimal point is relatively unchanged by differing porosities. The optimum present value becomes more defined with increasing porosity.

Impact of Reservoir Temperature on BHP Optimization Curve

The reservoir temperature affects both the phase equilibrium and the viscosity of the reservoir fluids. It is however a very well-known property, and there is very little uncertainty in its determination. Base case temperature is 250 °F.

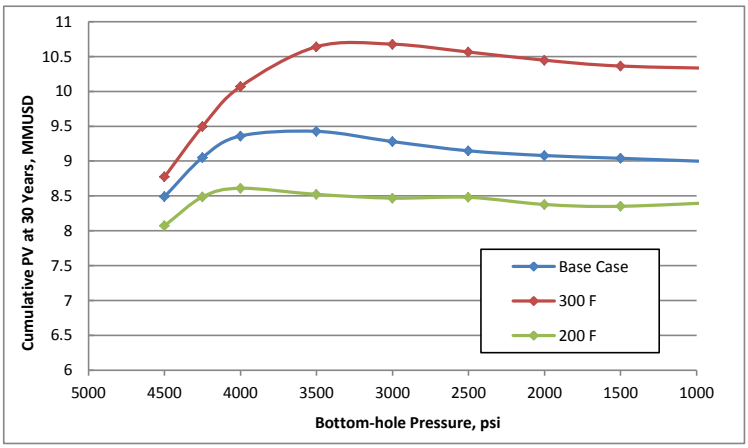

Figure 18: Impact of reservoir temperature on BHP optimization curve

The present value of the well stream tends to increase with increasing reservoir temperature. This effect is most pronounced at lower bottom-hole pressures. Increased temperature corresponds to a decreased retrograde dew point. This allows the drawdown to be larger whilst keeping single phase gas in the reservoir, as a result the optimum point moves to a lower BHP. A higher reservoir temperature also reduces the viscosity of the fluids and in particular increases the mobility of the liquid phase. This also works to reduce the optimum BHP as more fluids can be produced once critical oil saturation is reached.

Impact of Gas Relative Permeability Exponent on BHP Optimization Curve

The gas relative permeability curve determines how much of a barrier to gas flow liquid dropout is. The higher the exponent the more sharply the drop in relative permeability is for a given increase in liquid saturation in the matrix. Base case gas relative permeability exponent is 2.5.

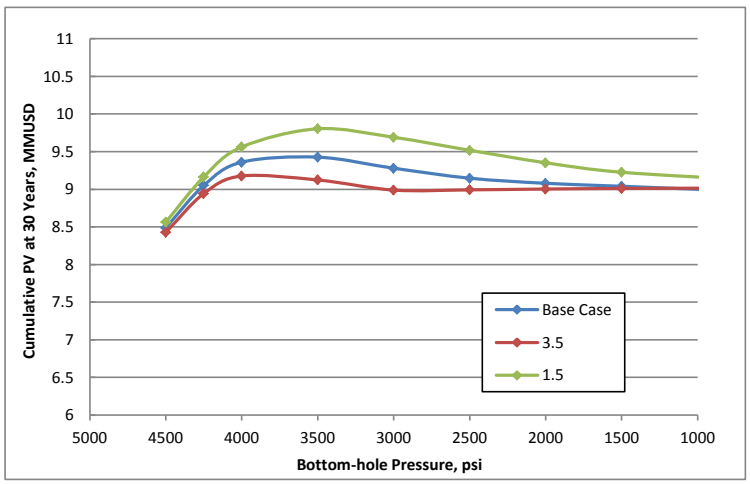

Figure 19: Impact of gas relative permeability exponent on BHP optimization curve

Higher gas relative permeability exponents correlate to lower present values. The optimum point shifts towards lower BHPs with decreasing gas exponent. This occurs as the gas becomes a larger factor in production.

Impact of Oil Relative Permeability Exponent on BHP Optimization Curve

The oil relative permeability curve determines the point at which liquid begins to flow. The higher the exponent, the more reluctant liquid is to flow through the rock, and the greater the stable saturation of liquid will be in the near fracture region. Base case oil relative permeability exponent is 8.

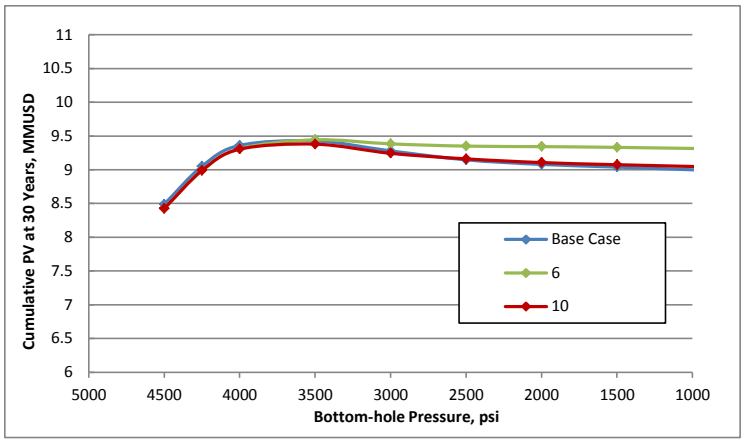

Figure 20: Impact of oil relative permeability exponent on BHP optimization curve

Increasing the oil relative permeability exponent above the base case value of 8 does not seem to affect production significantly. Lower exponents seem to increase production at sub-optimal BHPs, however the increase in optimal present value is negligible in the range represented here.

Impact of Fracture Conductivity on BHP Optimization Curve

The fracture conductivity was varied by altering the permeability of the cells occupied by the fracture. The same methods of assigning permeability were used as outlined in the gridding section. The base case fracture conductivity is 1 mD.ft.

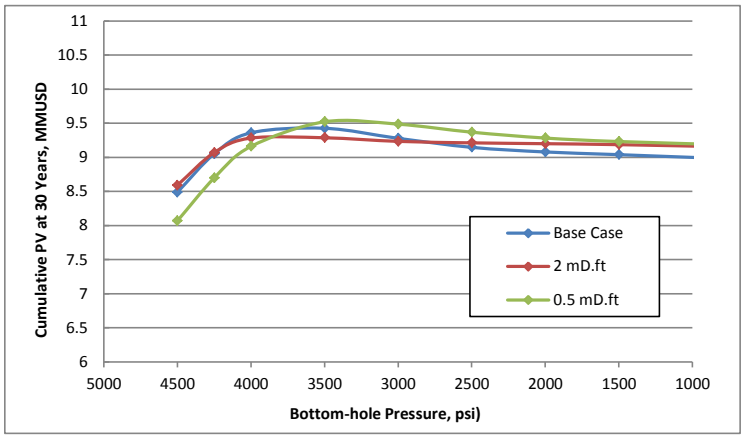

Figure 21: Impact of hydraulic fracture conductivity on BHP optimization curve

As fracture conductivity increases through the range simulated, the optimum point moves towards lower pressures. This in turn increases the present value at the optimum BHP. This could be caused by liquid dropout moving from the fracture – which has a linear relative permeability – to the matrix, which has a much more gas favourable relative permeability. This observation suggests the existence of optimal fracture conductivity. However, any application to reality would require verification through analysis of real completion and production data to establish a correlation.

Discussion

It is concluded that the optimal gridding technique for planar fracture models of liquid rich shale reservoirs is based on logarithmic refinement. In the model used in this study, the fracture is parallel to the j-direction. Because of this, flow dominates in the i-direction (towards the fracture face) and so refinement is most important in this direction. When simulating shale reservoirs it is important to capture the extreme pressure drops close to the fracture face. This need is even more important when dealing with liquids rich fluids. This is because close to the fracture face there can be dramatic changes in the extent of liquid dropout and therefore hydrocarbon mobility. A schematic of the pressure drop is shown in Figure E-2 which shows the grid block approximations for a uniform grid and a logarithmically refined grid. The pressure drop is particularly steep close to the well and using a uniform gridding approach is inefficient. Either the grid is too coarse to accurately capture the changes in liquid dropout close to the fracture face, or the grid is very fine, which captures the dropout well, but would contain far too many cells to be practical for simulation. The compromise is logarithmic refinement which allows cells to reduce in size close to the fracture. By employing symmetry element and only simulating one quarter of an individual fracture, the model can be simulated to a resolution of 0.25 ft thickness for the fracture cells while running in under 30 minutes.
An issue with logarithmic refinement is that when modelling a fracture of a given size, if logarithmic refinement is used in all directions – including the j-direction - the fracture cannot be represented explicitly. In order to address this problem cells that would contain the fractures edge were assigned a permeability calculated as a weighted average of the matrix and fracture permeabilities. This approach worked well within the context of this study as demonstrated in Figure 7. The simulations could differ from reality slightly in that no maximum rate restrictions were used, as demonstrated in Figure 8. This is unrealistic since the early time production values are enormous. This decision was made in the interests of keeping the model general, and in fact would cause an overestimation of low BHP production values since during early times the liquid dropout is not a dominating factor. It can therefore be concluded that this assumption does not affect the conclusion that these optimal points exist. Any effect on production values is assumed to be negligible since the simulations are run for 30 years and therefore dominated by late time behaviour.

Uncertainties are an obstacle to any shale modelling effort. This is in part due to the complex production systems that are exhibited, but also due to the heterogeneity and variations in fluid properties that can occur within the same formation. Total and relative permeabilities are extremely difficult to measure in shale, and data on them is sparse and sometimes unreliable. The motivation for conducting the sensitivity analysis given in the study is not only to look at the effect of reservoir parameters on production, but also to see their effect on the existence of the optimal point. Minimizing liquid dropout has many benefits, and reservoirs that have a defined optimum point may prove to have an advantage over those that do not. Although this study identifies the existence of an optimum bottom-hole flowing pressure, it must be noted that this optimum is a function of all the reservoir and fluid parameters. Identifying the fluid CGR is critical to optimizing the recovery, and as noted in (C. H. Whitson, 2012), fluid samples should be taken early on in the life of the well, and at as low a drawdown as possible to ensure as representative a sample as possible is collected.

The BHP optimization curves show that the present value of the well stream drops off sharply when the optimum point is exceeded, but reduces smoothly when it is underestimated. This observation suggests that it would prove more costly to overestimate the optimum bottom-hole pressure as this could leave it above the saturation pressure rather than just below it. It must however be remembered that losses due to liquid dropout are harder to regain due to the negligible relative permeability to condensate at low liquid saturations, so BHP should be reduced with caution.

The existence of an optimum point relies on the price ratio of gas to oil remaining low into the future. The author believes this to be a reasonable assumption for the United States given the surge of activity in shale gas. The optimum is still observed up to a ratio that would be equivalent to approximately 100 $/Bbl. and 4 $/MScf. Above this ratio the optimum point moves towards the lower bottom hole pressure. It is however important to realize that the optimum point could be shifted later in the life of the well. This could be as a result of greater knowledge of the reservoir through history matching of the well or other nearby wells, or because of changing oil-gas price ratios.

Some papers (T. Firincioglu, 2012; D. Devegowda, 2012) have argued that the extremely small pore sizes present in shale can actually affect the thermodynamics, wetting properties and phase behaviour of the fluids that they contain. Happily, one overriding effect that is predicted is dew point suppression which causes the phase envelope to shift towards lower pressures, thereby allowing higher drawdowns. If dew point suppression is present in reality the optimum points that are predicted in this study are likely to be pessimistic, as the effect of dew point suppression could allow lower BHPs to be implemented in practice effectively shifting the optimum point. However, dew point suppression would only apply to those fluids that are specifically held in the tiny pores <100 nm (T. Firincioglu, 2012). If there were any natural fractures present then it is likely that conventional thermodynamic behaviour would be observed. Naturally this applies to hydraulically stimulated fractures also.

Another effect that is a consequence of nano-scale pore sizes is the “molecular sieve” effect. Small molecules will pass

through the matrix more easily than larger molecules since large molecules have to decrease their effective length to pass through the smallest pores. It is difficult to predict the qualitative impact on revenue performance from this effect as it has opposing effects. Less large molecules reaching the wellbore will mean less liquid dropout and allow the use of lower BHPs. However, the fluid that reaches the wellbore and fractures will be leaner and therefore produce less oil at surface.

Attempts were made during the study to simulate using a near-critical fluid with a condensate gas ratio of 150 Stb/MMScf. It was found that although simulations at low BHPs ran, simulation became more difficult with increasing BHP up to the saturation pressure, approaching the critical point. The reasons for this are not precisely clear; however it is believed that this occurs as a result of the discontinuity in saturation that occurring in the near fracture face region. It seems that once this discontinuity has moved away from the fracture to the larger grid blocks the simulations becomes stable and can run. A recommendation for further work into the simulation of near critical fluids in liquid rich shales has been included below.

Suggestions for Further Work

1. A detailed uncertainty analysis is recommended to investigate how the uncertainty of reservoir and fluid properties could influence the optimal BHP. This study could make use of Monte Carlo simulations to predict the spread of production values if the optimum BHP is used. An analysis of possible future oil and gas prices could also be included. It is likely that such a study would require the use of 2 dimensional modelling and/or a black-oil fluid model so that the simulations could be run in reasonable time scales. The 2-D model would be representative of the behaviour of a full 3-D model. Although more rigorous, the modelling approach used in this study is too cumbersome to carry out the number of simulations that would be required for such a study. An uncertainty analysis such as described could ascertain whether the knowledge of the reservoir is known with enough certainty to implement this optimization. Such a study could also take opportunity to quantify the effects of using different equations of state such as Soave-Redlich-Kwong (SRK) and different viscosity models such as Lohrenz-Bray-Clark (LBC).
2. An investigation into the operation of liquid rich shale wells at low bottom-hole pressures is recommended. The aim of this work was to obtain the optimum bottom-hole pressures that minimized liquid dropout in the reservoir. It is however possible that increased revenue could be had by operating at lower bottom-hole pressures than those analysed here. Operating at low bottom-hole pressures in liquid rich shale systems brings with it a number of additional complexities. The Eagle Ford formation is comparatively soft, and so there is the problem of proppant embedment. This could be worsened by low bottom-hole pressures and compound the effect of drawdown sensitive fracture conductivity. High rock compressibility may also cause pressure sensitive permeability which may negatively impact production at low BHPs. An economic balance would exist in the design of the production tubing. A study which investigated the use of any existing lower optimal points would have to consider these effects as part of a modelling effort to justify operating at these lower bottom-hole pressures.
3. Further work on the applicability of pressure transient analysis to the characterization of liquids-rich shale reservoirs is recommended. A base case model could be used to simulate build up. Simulations could be run for varying reservoir properties and completions parameters as a parametric study. This would help gauge the importance of pressure transient analysis in characterizing liquids-rich shale reservoirs, and provide further justification for the collection of pressure transient data in future liquids-rich shale wells.
4. A simulation study into the “molecular sieve” effect predicted in shale is recommended. This effect was not included in this work, and as detailed in the discussion, its effect on production behaviour is difficult to qualify. Such a study would likely need to make use of detailed knowledge of the pore structure of shale, and attempt to model how different hydrocarbons are separated upon flow. The results from this study could then be applied to a large scale reservoir simulation to look at the impact this effect has on liquid dropout throughout the reservoir, fluid sampling analysis, and production revenue behaviour.
5. Further study into the optimization of blow down towards the end of well life is recommended. This study assumes constant bottom-hole pressures throughout the wells life, which is unrealistic in practice. Although drawing down at very low pressure is detrimental in the long term, it is likely that towards the very end of the wells life, it would be economical to allow the well to flow at the minimum bottom-hole pressure.
6. A gridding study is recommended into the simulation of near critical fluids in ultra-low permeability reservoirs. It is thought that logarithmic refinement towards the fracture face does not deal well with the near-discontinuity in saturation that occurs near the critical point. It may be necessary to experiment with variable refinement factors or other refinement schemes in order to be able to simulate these kinds of fluids within reasonable timescales. There may also be analytical approaches that could be used to define the pressures in blocks undergoing critical phase change.

Conclusions

This study identifies the presence of an optimal bottom-hole flowing pressure (BHP) for producing from liquids-rich shale reservoirs with condensate gas ratios of 30 and 75 Stb/MMScf. The optimum BHP maximises revenue over the life of the well, whilst minimizing liquid dropout in the reservoir. Some of the main conclusions that may be drawn from this work are summarized below:

- Logarithmic gridding is particularly useful in the modelling of liquid rich shale systems in order to accurately capture the liquid dropout effects and steep pressure gradients in the near fracture region. In particular the refinement in the direction towards the fracture face is most important.

  The long term production behaviour of a planar fracture refined to the tip and the well block can be replicated by using permeability approximations for the fracture edge cells while refining to the well block alone.
- Condensate gas ratio of the well stream reduces as the flowing bottom hole pressure is reduced. This is due to a larger degree of liquid dropout occurring in the reservoir.
- Drawing down at minimum bottom-hole pressure does not necessarily maximize the present value, and may in fact damage the reservoir permanently. Optimal bottom-hole pressures tend to still be below the saturation pressure, so some dropout is necessary in order to optimize revenue. This is however dependant on the parameters used in this study, and some systems may show optimal points at or closer to the dew point.
- It is important to take care when simulating in systems where the reservoir conditions are close to the critical point of the fluid. It may be necessary to explore new refinement schemes when working with these types of systems, as the steep pressure gradients in shale can compound the difficulty in simulating them.
- Identifying the optimal point with accuracy relies on a confident knowledge of the reservoir parameters, and of the fluid properties. History matching and/or pressure transient analysis of similar wells is required to further knowledge before these workflows can be implemented, to avoid the over estimation of the optimal bottom-hole pressure.
- The optimum point is extremely sensitive to the fluid CGR, it is therefore of utmost importance that the in-situ fluid is characterized accurately in order to arrive at representative values of optimal bottom-hole pressures, and to understand the potential for condensate blocking damage in the reservoir.
- The production values quoted in this study are likely to be pessimistic for the chosen base case parameters. The phenomena of dew point suppression and adsorption may in fact reduce liquid dropout in reality, and as a result it may be possible that the true optimal bottom-hole pressure is lower that the methods used in this work would suggest.

These conclusions are arrived at as a result of the chosen base case parameters and methods of calculation. It is not the aim of the study to identify optimal points quantitatively, only to identify their plausibility in a proof-of-concept manner, and assess their behaviour under moderately variable reservoir conditions. A quantitative calculation of well optimization is beyond the scope of this study, and would require detailed analysis of the system. Any conclusions reached would again be a function of the data and assumptions used in such a study.

Note on Software Used

This study used the Computer Modelling Group (CMG) GEM package for all reservoir simulation. CMG GEM is a general equation-of-state compositional simulator. PVTSim was used for all PVT analysis. PVTSim is a general equation-of-state based PVT simulator.

Abbreviations

LR-FF-FT: Logarithmic refinement to both fracture tip and fracture face
LR-FF: Logarithmic refinement to fracture face only
BHP: Bottom-hole pressure
CGR: Condensate Gas Ratio expressed in Stb/MMScf
USD: US Dollars
PV: Present Value

Unit Conversion Factors

psi x 6.894 757 E+00	=	kPa	(°F+459.67)/1.8	=	K
bbl x 1.589 873 E-01	=	m^3	ft x 3.048 E-02	=	m
cf x 2.831 685 E-02	=	m^3	in x 2.54 E+00	=	cm
(°F-32)/1.8	=	°C	acre x 4.046873 E+03	=	m^2

References

A. Inamdar, R. M. (2010). *"Evaluation of Stimulation Techniques Using Microseismic Mapping in the Eagle Ford Shale" Paper SPE 136873 prepared for presentation at the SPE Tight Gas Completions Conference, San Antonio, Texas, USA 2-3 November.* SPE.

A. Orangi, N. R. (2011). *"Unconventional Shale Oil and Gas-Condensate Reservoir Production, Impact of Rock, Fluid and Hydraulic Fractures" Paper SPE 140536 prepared for presentatiion at the SPE Hydraulic Fracturing Technology Conference and Exhibition, The Woodlands, Texas, USA, 24-26 January.* SPE.

A. S. Chaudhary, C. E.-E. (2011). *"Shale Oil Production Performance from a Stimulated Reservoir Volume" Paper SPE 147596 prepared for presentation at the SPE Annual Technical Conference and Exhibition, Denver, Colorado, USA, 30 Oct - 2 Nov 2011.* SPE.

C&C Reservoirs. (2011). *Eagle Ford Shale Play - Field Evaluation Report.* C&C Reservoirs.

C. H. Whitson, S. S. (2012). *"PVT in Liquid-Rich Shale Reservoirs" Paper SPE 155499 prepared for presentation at the SPE Annual Technical Conference and Exhibition, San Antonio, Texas, USA, 9-10 October.* SPE.

D. Devegowda, K. S. (2012). *"Phase Behavior of Gas Condensates in Shales Due to Pore Proximity Effects: Implications for Transport, Reserves and Well Productivity" Paper SPE 160099 prepared for presentation at the SPE Annual Technical Conference and Exhibition, San Antonio, Texas, USA .* SPE.

D. Ilk, N. J. (2012). *"Production Analysis in the Eagle Ford Shale - Best Practices for Diagnostic Interpretations, Analysis, and Modeling" Paper SPE 160076 prepared for presentation at the SPE Annual Technical Conference and Exhibition, San Antonio, Texas, USA, 8-10 October.* SPE.

EOG Resources. (2011). *South Texas Eagle Ford Play Summary.* EOG Resources.

J. Mullen, S. H. (2010). *"Petrophysical Characterization of the Eagle Ford Shale in South Texas" Paper CSUG/SPE 138145 prepared for presentation at the Canadian Unconventional Resources & International Petroleum Conference, Calgary, Alberta, Canada 19-21 October.* SPE, CSUG.

J. Wan, R. S.-D. (2013). *"Factors Controlling Recovery in Liquids Rich Unconventional Systems" Paper IPTC 17103 prepared for presentation at the International Petroleum Technology Conference, Beijing, China, 26-28 March 2013.* IPTC, SPE.

L. Fan, R. M. (2011). *"An Integrated Approach to Understanding Oil and Gas Reserves Potential in the Eagle Ford Shale Formation" Paper CSUG/SPE 148751 prepared for presentation at the Canadian Unconventional Resources Conference, Calgary, Alberta, Canada, 15-17 November.* CSUG/SPE.

R. Shelley, L. S.-T. (2012). *"Understanding Hydraulic Fracture Stimulated Horizontal Eagle Ford Completions" Paper SPE 152533 prepared for presentation at the SPE/EAGE European Unconventional Resources Conference and Exhibition, Vienna, Austria, 20-22 March.* SPE.

Rubin, B. (2010). *"Accurate Simulation of Non Darcy Flow in Stimulated Fractured Shale Reservoirs" Paper SPE 132093 prepared for presentation at the SPE Western Regional Meeting, Anaheim, California, USA, 27-29 May 2010.*

Schlumberger. (2009). *Flow Scanner Interpretation Results - Well Briscoe G#1H Eagle Ford, Texas, USA.*

Swindell, G. S. (2012). *"Eagle Ford Shale - An Early Look at Ultimate Recovery" Paper SPE 158207 prepared for presentation at the SPE Annual Technical Conference and Exhibition, San Antonio, Texas, USA, 8-10 October 2012.* SPE.

T. Firincioglu, E. O. (2012). *"Thermodynamics of Multiphase Flow in Unconventional Liquids-Rich Reservoirs" Paper SPE 159869 prepared for presentation at the SPE Annual Technical Conference and Exhibition, San Antonio, Texas, USA.* SPE.

Appendices

Appendix A: Critical Milestones

SPE Paper Number	Year	Title	Authors	Contribution
7921	1979	Gas Occurrence in the Devonian Shale	E.C. Smith S. P. Cremean G. Kozair	First to conclude that the matrix is the major source of produced gas in shale gas reservoirs
125530	2009	Reservoir Modelling in Shale-Gas Reservoirs	C.L. Cipolla E.P Lolon J.C. Erdle B. Rubin	Discusses various simulation approaches, focusing on the impact of gas desorption and stress sensitive fracture conductivity
132093	2010	Accurate Simulation of Non-Darcy Flow in Stimulated Fractured Shale Reservoirs	B. Rubin	A method of simulating non Darcy flow accurately using models that run on the time scale of minutes on modern computers
140536	2011	Unconventional Shale Oil and Gas-Condensate Reservoir Production, Impact of Rock, Fluid, and Hydraulic Fractures	A. Orangi N. R. Nagarajan M. M. Honarpour J. Rosenweig	Analyses the effect of various reservoir and fluid parameters on production using grid based modelling
155499	2012	PVT in Liquid Rich Shale Reservoirs	C.H. Whitson S. Sunjerga	Investigates the variation in production rate as a function of the PVT properties of the reservoir fluid
158042	2012	Characterization of Critical Fluid, Rock, and Rock-Fluid Properties – Impact on Reservoir Performance of Liquid-Rich Shales	M. M. Honarpour N. R. Nagarajan A. Orangi F. Arasteh Z. Yao	Formulated a methodology for characterizing rock and fluid properties for LRS reservoirs, and their impact on performance
159869	2012	Thermodynamics of Multiphase Flow in Unconventional Liquids – Rich Reservoirs	T. Firincioglu E. Ozkan C. Ozgen	Demonstrated that the capillary and surface forces in nano – Darcy permeability rock affect phase behaviour significantly
160099	2012	Phase Behaviour of Gas Condensates in Shales Due to Pore Proximity Effects: Implications for Transport, Reserves and Well Productivity	D. Devegowda K. Sapmanee F. Civan R. Sigal	Suggests a quantitative approach to modelling the physical phenomena in nano scale porosity reservoirs that can affect production performance
163651	2013	Beyond Dual-Porosity Modelling for the Simulation of Complex Flow Mechanisms in Shale Reservoirs	B. Yan Y. Whang J. Killough	First to apply a five aspect micro scale model to simulate production from shale
163990	2013	On Simulation of Flow in Tight and Shale Gas Reservoirs	A. Darishchev P. Lemouzy P. Rouvroy	Sensitivity study on effect of stimulated reservoir volume on production, and comparisons of dual porosity-permeability models

Table A-1: Critical milestones

Appendix B: Base Case Parameters

Parameter		Units	Source
Wellbore Diameter	5.5	inches	2, 10
TVD	10000	ft	1, 10
Thickness	200	ft	1, 2, 11
Lateral Spacing	660	ft	1*, 3
Drainage Area	80	ac.	3, 8*
Lateral Length	5000	ft	1, 2, 10
Number of Stages	12	-	1, 8, 10
Clusters Per Stage	4	-	1, 8, 10
Frac Spacing	105	ft	2*, (and 1, 8, 10)
Frac Half Length Horizontal	75	ft	3*, 8
Frac Half Length Vertical	50	ft	3*
Matrix Porosity (effective)	9	%	1, 7, 11
Fracture Aperture	0.00018	inch	4
Fracture Spacing	0.135	inch	4
Fracture Porosity	0.001	-	-
Matrix Permeability Horizontal	320	nD	1, 7, 9*, 11
Matrix Permeability Vertical	32	nD	1*, 9
Fracture Permeability Horizontal	320	nD	-
Fracture Permeability Vertical	32	nD	-
Hydraulic Fracture Width	0.001	ft	6
Hydraulic Fracture Permeability	1000	mD	8
Hydraulic Fracture Conductivity	1	mD.ft	-
Initial Reservoir Pressure	7000	psia	1, 7
Reservoir Temperature	250	F	1, 9
Rock Compressibility	25	microsip	5,6
Recovery Factor	25	%	1, 8
Well Life	30	years	8*

Table B-1: Parameters chosen for use in base case model

(*within range of values found in source)

Number	Reference
1	(C&C Reservoirs, 2011)
2	(L. Fan, 2011)
3	(A. Inamdar, 2010)
4	(J. Mullen, 2010)
5	(A. S. Chaudhary, 2011)
6	(A. Orangi, 2011)
7	(EOG Resources, 2011)
8	(D. Ilk, 2012)
9	(Schlumberger, 2009)
10	(Schlumberger, 2009)
11	(R. Shelley, 2012)

Table B-2: Reference key for sources cited in Table 1

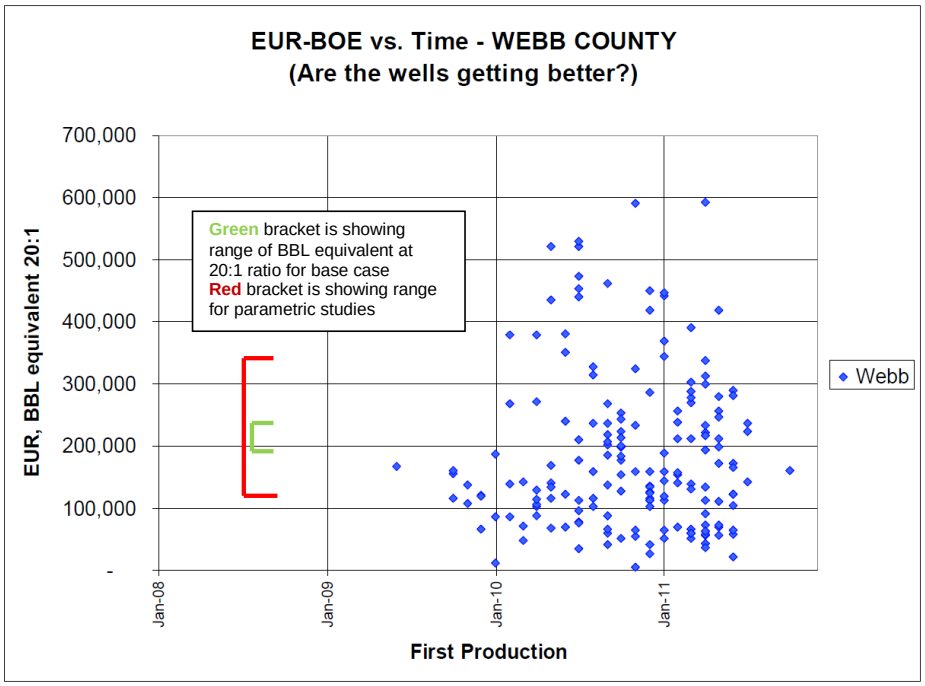

Figure B-1: Estimated ultimate recovery vs. first production date for Eagle Ford wells (Swindell, 2012)

Appendix C: PVT

Three fluids were used in this study with CGRs of 30, 75 and 150. The following data for these fluids was used in the compositional model and was adapted from (C. H. Whitson, 2012).

Compositions

Component	CGR 30	CGR 75	CGR 150
N2	0.190	0.190	0.180
CO2	2.890	2.820	2.710
C1	72.420	70.660	67.910
C2	9.260	9.040	8.690
C3	5.180	5.060	4.860
I-C4	1.190	1.160	1.120
N-C4	2.040	1.990	1.910
I-C5	0.930	0.910	0.880
N-C5	1.000	0.980	0.940
C6	1.420	1.390	1.330
C7	1.090	1.280	1.690
C8	0.792	1.060	1.480
C9	0.517	0.792	1.170
C10	0.347	0.608	0.948
C11	0.233	0.467	0.768
C12	0.157	0.359	0.623
C13	0.106	0.276	0.506
C14	0.072	0.213	0.411
C15	0.049	0.165	0.335
C16	0.033	0.128	0.273
C17	0.023	0.099	0.223
C18	0.016	0.077	0.182
C19	0.011	0.060	0.149
C20	0.0075	0.047	0.123
C21	0.0052	0.037	0.101
C22	0.0036	0.029	0.083
C23	0.0025	0.023	0.069
C24	0.0018	0.0178	0.057
C25	0.0012	0.0140	0.047
C26+	0.0030	0.0554	0.240

Table C-1: Compositions of fluids CGR 30, CGR 75 and CGR 150

Equation of State Parameters Used in Fluid Model

Component	M	Tc (R°)	Pc (psia)	ω	Tb (R°)	SG	LBC Zc	Binary Interaction Parameters		
								H2S	N2	CO2
N2	28.01	227.2	492.8	0.037	139.4	-	0.292	-	-	-
CO2	44.01	547.4	1069.5	0.225	333.3	-	0.274	-	-	-
C1	16.04	343.0	667.0	0.011	201.6	-	0.286	0.08	0.02	0.12
C2	30.07	549.6	706.6	0.099	332.7	-	0.279	0.07	0.06	0.12
C3	44.10	665.7	616.1	0.152	416.2	-	0.276	0.07	0.08	0.12
I-C4	58.12	734.1	527.9	0.186	471.1	-	0.282	0.06	0.08	0.12
N-C4	58.12	765.2	550.6	0.200	491.1	-	0.274	0.06	0.08	0.12
I-C5	72.15	828.7	490.4	0.229	542.4	-	0.272	0.06	0.08	0.12
N-C5	72.15	845.5	488.8	0.252	557.0	-	0.268	0.06	0.08	0.12
C6	82.42	924.0	490.0	0.238	606.4	0.703	0.249	0.05	0.08	0.12
C7	96.05	990.6	454.2	0.274	661.0	0.737	0.278	0.03	0.08	0.10
C8	108.89	1043.4	421.4	0.311	707.5	0.758	0.271	0.03	0.08	0.10
C9	122.04	1093.5	388.5	0.351	754.1	0.775	0.264	0.03	0.08	0.10
C10	134.96	1138.0	360.3	0.391	797.0	0.788	0.258	0.03	0.08	0.10
C11	147.80	1178.2	335.6	0.431	836.9	0.800	0.253	0.03	0.08	0.10
C12	160.55	1214.9	314.0	0.470	874.4	0.809	0.249	0.03	0.08	0.10
C13	173.19	1248.7	294.9	0.508	909.6	0.818	0.245	0.03	0.08	0.10
C14	185.74	1279.8	278.1	0.546	942.7	0.826	0.242	0.03	0.08	0.10
C15	198.18	1308.7	263.2	0.583	974.0	0.833	0.238	0.03	0.08	0.10
C16	210.51	1335.5	249.9	0.620	1003.5	0.839	0.236	0.03	0.08	0.10
C17	222.73	1360.6	238.0	0.656	1031.5	0.845	0.233	0.03	0.08	0.10
C18	234.83	1384.1	227.2	0.691	1058.0	0.850	0.231	0.03	0.08	0.10
C19	246.83	1406.2	217.6	0.725	1083.2	0.855	0.229	0.03	0.08	0.10
C20	258.71	1427.0	208.8	0.759	1107.1	0.860	0.227	0.03	0.08	0.10
C21	270.48	1446.7	200.9	0.792	1129.9	0.865	0.226	0.03	0.08	0.10
C22	282.14	1465.3	193.6	0.824	1151.6	0.869	0.224	0.03	0.08	0.10
C23	293.69	1483.0	187.0	0.856	1172.4	0.873	0.223	0.03	0.08	0.10
C24	305.13	1499.8	180.9	0.887	1192.2	0.877	0.222	0.03	0.08	0.10
C25	316.47	1515.8	175.3	0.918	1211.2	0.880	0.221	0.03	0.08	0.10
C26+	412.23	1631.4	140.8	1.162	1349.7	0.906	0.217	0.03	0.08	0.10

Table C-2: Component properties and equation of state parameters used in fluid model

Phase Diagrams

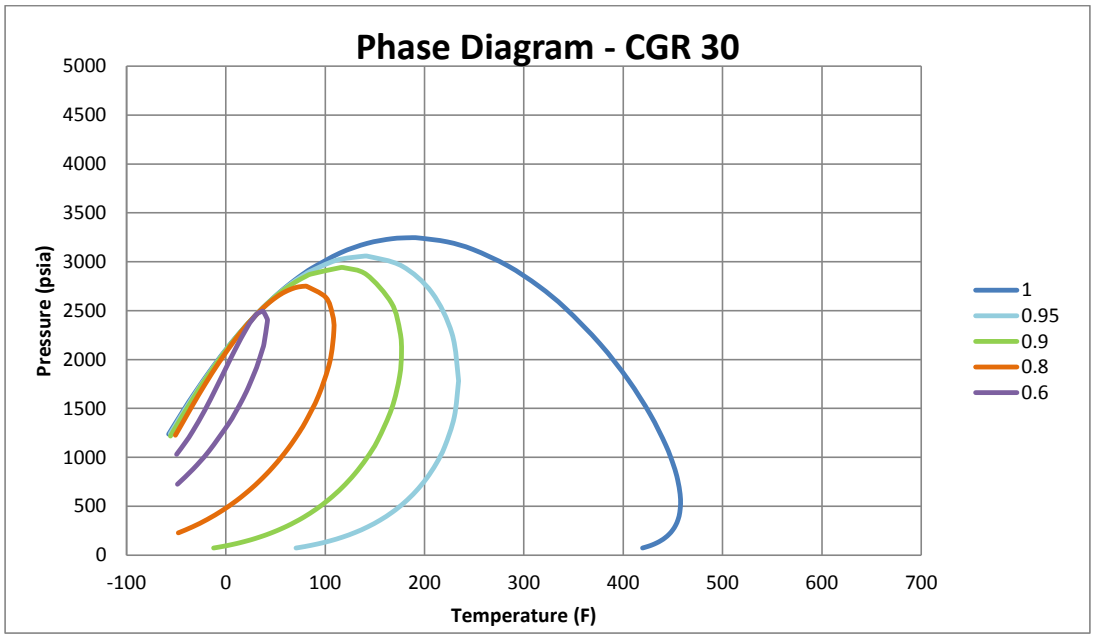

Figure C-1: Phase diagram – CGR 30 fluid

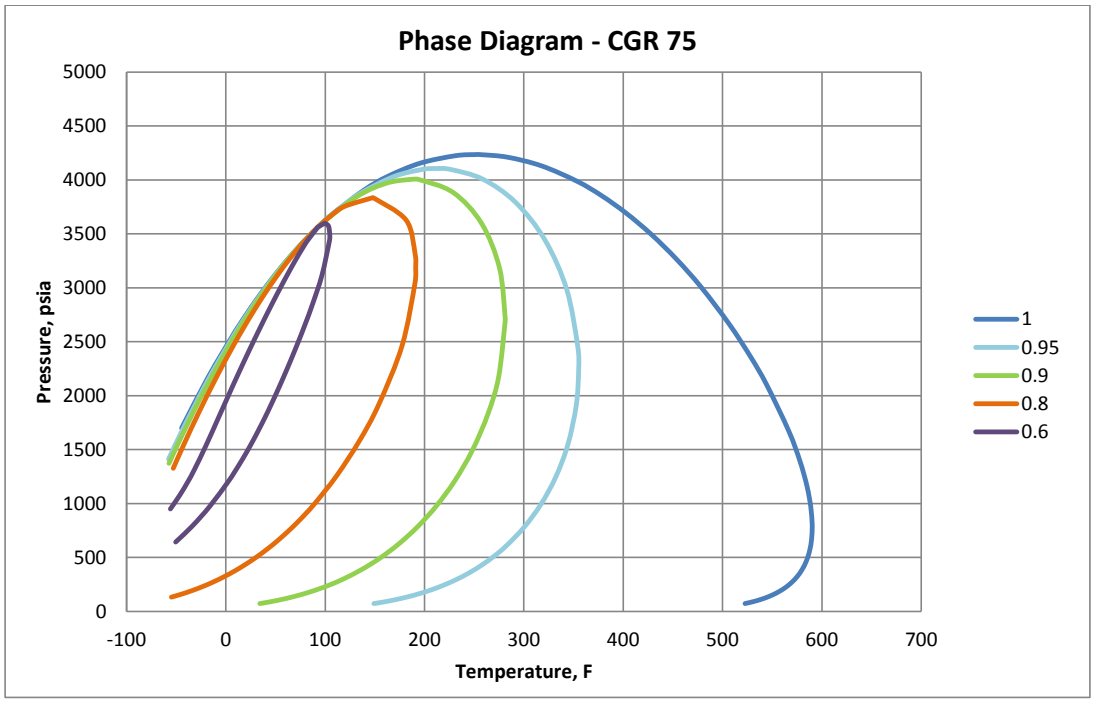

Figure C-2: Phase diagram – CGR 75 Fluid

Phase Diagrams Continued

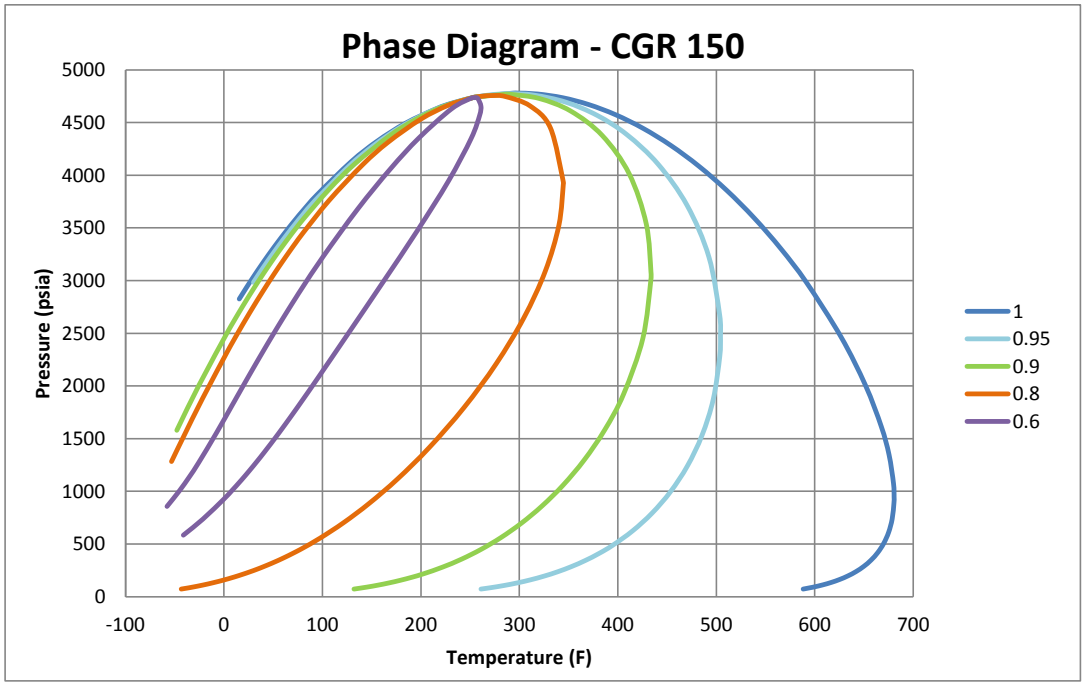

Figure C-3: Phase diagram – CGR 150 Fluid

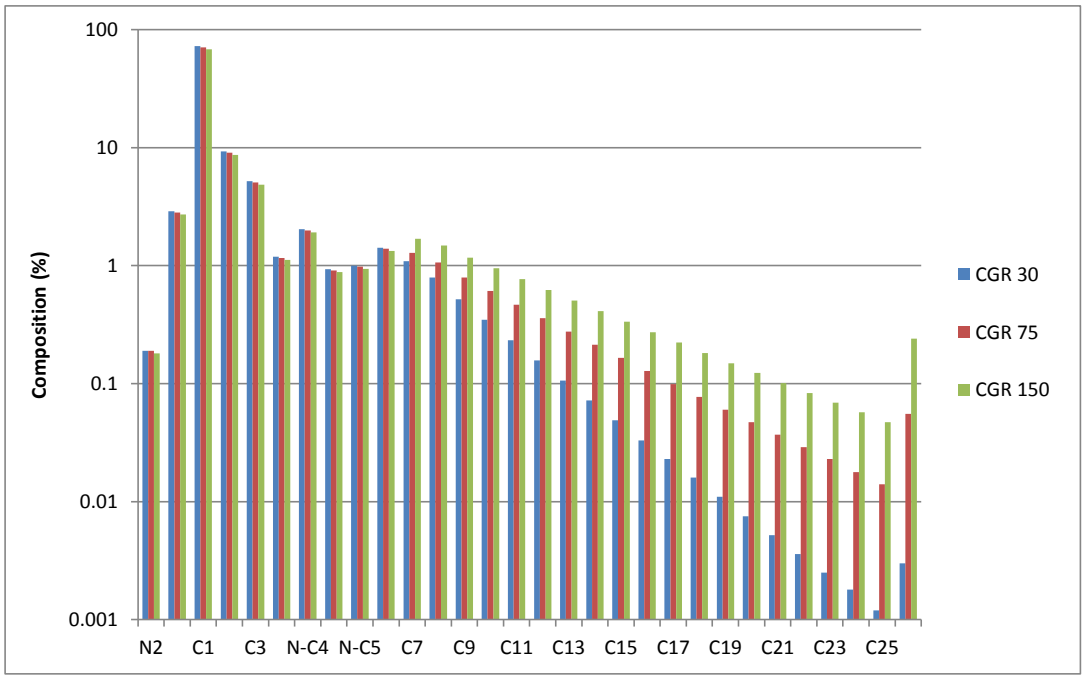

Figure C-4: Compositions of CGRs 30. 75 and 150 in comparison

Appendix D: Relative Permeability

Code	Description	Value
SWCON	Endpoint Saturation: Connate Water	0.4
SWCRIT	Endpoint Saturation: Critical Water	0.4
SOIRW	Endpoint Saturation: Irreducible Oil for Water-Oil Table	0.25
SORW	Endpoint Saturation: Residual Oil for Water-Oil Table	0.25
SOIRG	Endpoint Saturation: Irreducible Oil for Gas-Liquid Table	0
SORG	Endpoint Saturation: Residual Oil for Gas-Liquid Table	0.2
SGCON	Endpoint Saturation: Connate Gas	0.05
SGCRIT	Endpoint Saturation: Critical Gas	0.05
KROCW	Kro at Connate Water	0.6
KRWIRO	Krw at Irreducible Oil	0.8
KRGCL	Krg at Connate Liquid	0.6
KROGCG	Krog at Connate Gas	-
NKRW	Exponent for calculating Krw from KRWIRO	2
NKROW	Exponent for calculating Krow from KROCW	8
NKROG	Exponent for calculating Krog from KROGCG	8
NKRG	Exponent for calculating Krg from KRGCL	2.5

Table D-1: Three-phase relative permeability parameters used in the base case model

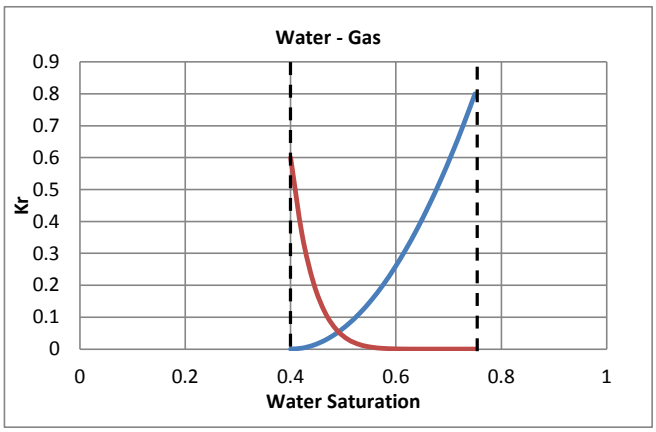

Figure D-1: Water – gas relative permeability curves

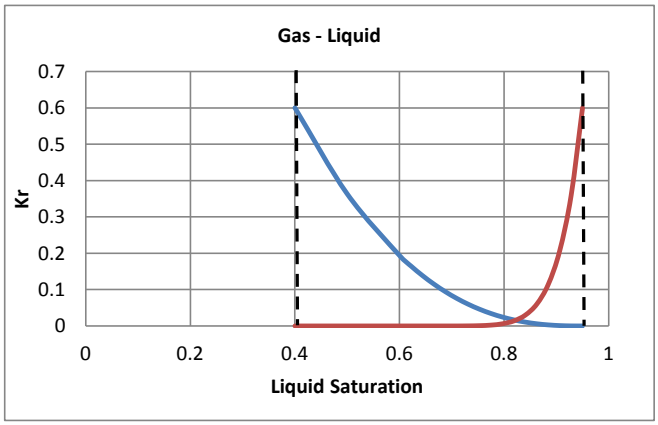

Figure D-2: Gas – liquid relative permeability curves

Appendix E: Gridding

Schematic of Grid Geometry

The following schematic shows the geometry of the model. A quarter symmetry element such as the one used in the BHP optimization studies is represented in blue.

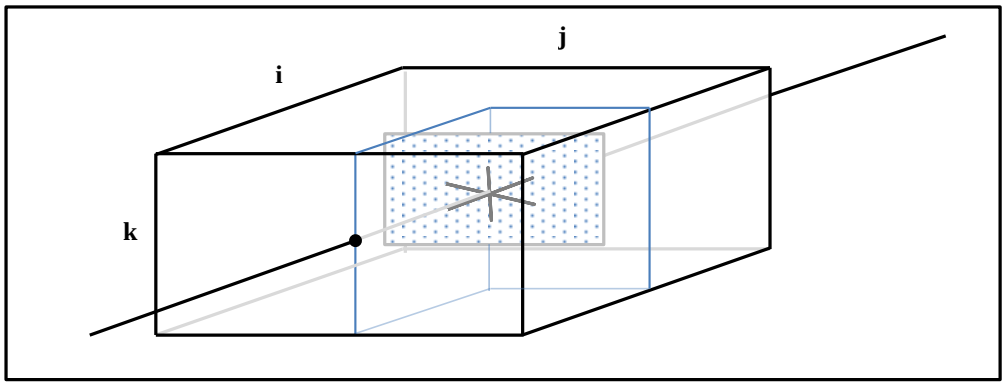

Figure E-1: Schematic of model geometry showing an entire fracture and no flow boundaries

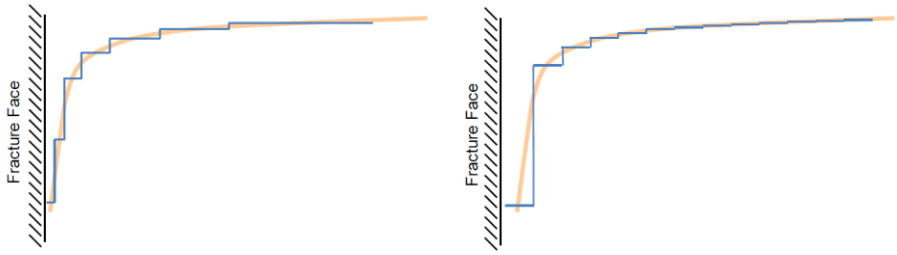

Figure E-2: Schematic of pressure profiles for logarithmic refinement and uniform gridding

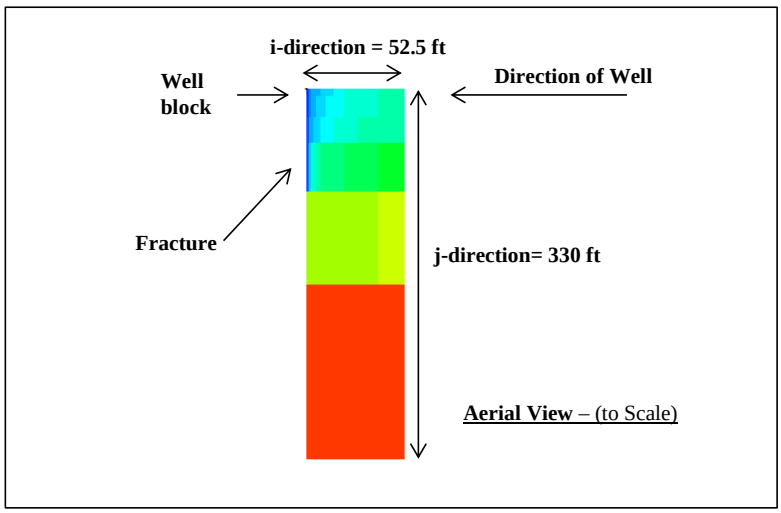

Figure E-3: Description of grid model showing orientation and well block placement

Quarter Grid Sizing

	Number of Cells in i-direction					All	
	16	14	12	10	8		
	i	i	i	i	i	j	k
Size of cells in the i-direction, ft	12.179	14.195	14.357	20.472	25.499	155.929	48.196
	9.398	10.407	9.936	12.549	13.177	82.375	25.093
	7.253	7.629	6.876	7.692	6.810	43.518	13.064
	5.597	5.593	4.759	4.715	3.519	22.990	6.802
	4.319	4.101	3.293	2.890	1.818	12.145	3.541
	3.333	3.006	2.279	1.772	0.940	6.416	1.844
	2.572	2.204	1.577	1.086	0.486	3.390	0.960
	1.985	1.616	1.092	0.666	0.251	1.791	0.500
	1.532	1.185	0.755	0.408	0.486	0.946	0.960
	1.182	0.868	0.523	0.250	0.940	0.500	1.844
	0.912	0.637	0.362	0.408	1.818	0.946	3.541
	0.704	0.467	0.250	0.666	3.519	1.791	6.802
	0.543	0.342	0.362	1.086	6.810	3.390	13.064
	0.419	0.251	0.523	1.772	13.177	6.416	25.093
	0.323	0.342	0.755	2.890	25.499	12.145	48.196
	0.250	0.467	1.092	4.715	-	22.990	-
	0.323	0.637	1.577	7.692	-	43.518	-
	0.419	0.868	2.279	12.549	-	82.375	-
	0.543	1.185	3.293	20.472	-	155.929	-
	0.704	1.616	4.759	-	-	-	-
	0.912	2.204	6.876	-	-	-	-
	1.182	3.006	9.936	-	-	-	-
	1.532	4.101	14.357	-	-	-	-
	1.985	5.593	-	-	-	-	-
	2.572	7.629	-	-	-	-	-
	3.333	10.407	-	-	-	-	-
	4.319	14.195	-	-	-	-	-
	5.597	-	-	-	-	-	-
	7.253	-	-	-	-	-	-
	9.398	-	-	-	-	-	-
	12.179	-	-	-	-	-	-

Table E-1: Dimensions used in the grid block size optimization study

Appendix F: Simulation Results

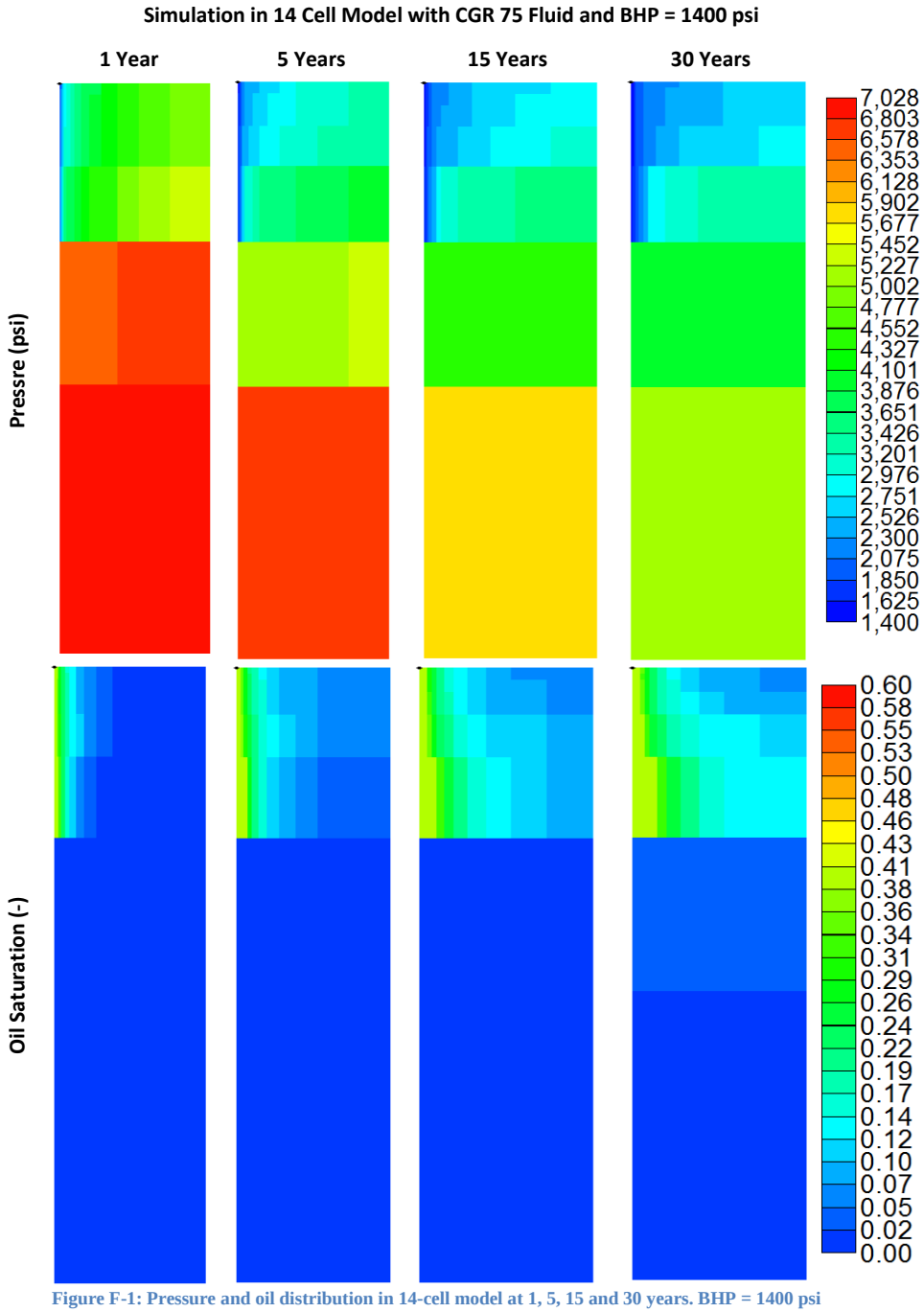

Figure F-1: Pressure and oil distribution in 14-cell model at 1, 5, 15 and 30 years. BHP = 1400 psi

Appendix G: Literature Review

SPE 155499 (2012)

PVT in Liquids Rich Shale Reservoirs

Authors: C.H. Whitson, S. Sunjerga

Contribution:

- Recommended practices for sampling, lab PVT tests, PVT model development and estimation of the in situ fluid system. Shows the variation of the Oil Gas Ratio (OGR) with time from Liquids-Rich Shale (LRS) wells.
- Methodology to estimate in situ reservoir fluid composition through the use of constant composition expansion tests

Objective:

- To address the sampling and PVT modelling of liquid-rich fluids produced from ultra-tight formations – Liquid Rich Shales (LRS) reservoirs.

Methodology Used:

- High resolution**,** finite difference, single well model using black oil and EOS PVT formulations.

Conclusions Reached:

- Best method for fluid sampling is early with low drawdowns.
- Equation of State (EOS) model is needed to generate reliable and consistent black oil PVT tables.
- Liquid yield (r_p) remains approximately constant for extended periods of time in LRS wells when the flowing BHP is fixed.
- Relative permeability and oil PVT properties have little to no effect on gas-condensate LRS wells whereas they do affect oil LRS wells

SPE 163990 (2013)

On Simulation of Flow in Tight and Shale Gas Reservoirs

Authors: A. Darishchev, P. Lemouzy, P. Rouvroy

Contribution:

- Advanced the understanding of hydraulic fracture network complexity.
- A sensitivity analysis on the variation of gas production with varying stimulated reservoir volume, matrix permeability.
- Comparison of the 2φ-2K model and the 2φ-1K model

Objective: To investigate the applicability of existing numerical simulation techniques to unconventional reservoirs.

Methodology Used:

- Numerical reservoir simulation
- Spatially and temporary varied properties such as fracture permeability

Conclusions Reached:

- A multidisciplinary approach is valuable in the successful development of unconventional reservoirs
- The applicability of dual medium simulation approaches requires further investigation and research

Comments:

- Considers dry gas production only

SPE 140536 (2011)

Unconventional Shale Oil and Gas-Condensate Reservoir Production, Impact of Rock, Fluid and Hydraulic Fractures

Authors: A. Orangi, N.R. Nagarajan, M.M. Honarpour, J. Rosenweig

Contribution: Showed how cumulative production varies with various rock and fluid parameters:

- Fluid condensate gas ratio (CGR)
- Rock Compressibility
- Relative permeability Corey exponent
- Critical gas saturation
- Critical condensate saturation
- Surface area of contact (SAC)
- Fracture permeability

Objective: To investigate the impact of rock and fluid properties and the drainage area of hydraulically fractured wells in a standard development pattern

Methodology Used: Numerical compositional reservoir modelling, sensitivity analyses

Conclusions Reached:

- All of the tested variables are critical to unconventional reservoir performance prediction
- Matrix away from the fractures remains relatively constant pressure throughout entire depletion >30 years
- Liquid recovery is optimum for CGR = 200 – 300 stb/MMscf
- High rock compressibility is detrimental to both gas and liquids production
- Fracture surface area is the major parameter affecting cumulative production
- Fracture conductivity can be lost during depletion impacts production severely
- Fracture interference is limited and may only occur late in reservoir life

Comments

- Does not investigate the effects of the operating strategy/pressure regime on cumulative production.
- Only varies CGR and does not consider the effects of liquid dropout on both gas and condensate production

IPTC 17103 (2013)

Factors Controlling Recovery in Liquids Rich Unconventional Systems

Authors: J. Wan, R.S. Barnum, D.C. DiGloria, A. Leahy-Dios, R. Missman, J. Hemphill

Contribution:

- A discussion of the factors that control recovery in liquids rich unconventional systems, in particular shale.
- A deeper understanding of how liquid dropout in gas condensate shale is influenced by the initial reservoir pressure, and how relative permeability effects in turn affect liquid production

Objective: To enhance the understanding of the impact phase behaviour has on the performance of liquid rich systems, specifically investigate how liquid yield effects rate and recovery.

Methodology Used:

- Compositional modelling
- Single fracture model

Conclusions Reached:

- Geology and phase behaviour are critical
- Composition of in place fluids, their phase behaviour and initial reservoir conditions are important factors

SPE 163651 (2013)

Beyond Dual-Porosity Modelling for the Simulation of Complex-Flow Mechanisms in Shale Reservoirs

Authors: B. Yan, Y. Wang, J.E. Killough

Contribution:

- Presents a new multi scale porosity model by considering three separate porosity systems: organic matter, inorganic matter, and natural fractures
- Incorporates the presence of vugs in kerogen

Objective:

- To improve on conventional dual porosity/permeability models

Methodology Used:

- Numerical simulation
- Individual grid cells are assigned a type from the following four continua: Nano pore (organic), Vug (organic), Inorganic (rock), Fracture. These are then used to construct the matrix block system.
- Monte Carlo simulations determine the concentration of organic grid units dispersed in the matrix

Conclusions Reached:

- The new model gives results which differ significantly from the conventional dual porosity/permeability model
- Diffusion cannot be neglected
- Although gas desorption provides gas in place and can sustain higher cumulative production, it does little to alter the gas drainage capacity of the reservoir model

SPE 159869 (2012)

Thermodynamics of Multiphase Flow in Unconventional Liquids – Rich Reservoirs

Authors: T. Firincioglu, E. Ozkan, C. Ozgen

Contribution:

- Recognises the importance of considering surface effects on the PVT behaviour of liquid rich reservoir fluids in ultra-tight permeability reservoirs

Objective:

- To investigate the effect that capillary and surface disjoining force interactions - such as van der Waals, structural and adsorption – have on macroscopic phase behaviour.

Methodology Used:

- Three unconventional oil samples studied
- Peng Robinson Equation of State (PR EOS) used with modified Vapour Liquid Equilibrium calculations to include capillary and surface forces.

Conclusions Reached:

- Capillary discontinuities and surface forces in nano pores of liquids rich reservoirs cause significant deviation from conventional phase behaviour
- VLE condition for the first gas bubble places restrictions on pore sizes that bubbles can form in a closed system
- Gas composition at bubble point depends on the suppression value, and therefore on the pore size, this impacts gas phase growth and could cause flow due to diffusion
- For a confined fluid, the under saturated portion of the formation volume factor curve extends further into low pressure range

SPE 132093 (2010)

Accurate Simulation of Non-Darcy Flow in Stimulated Fractured Shale Reservoirs

Authors: B. Rubin

Contribution:

- A technique to accurately model fractures within a stimulated reservoir volume (SRV) that uses a logarithmically spaced, locally refined dual permeability approach, or a LS-LR-DK grid.

Objective:

- To produce predictive shale gas simulation models that are simple and can be run in minutes as opposed to hours or days

Methodology Used:

- High resolution reference models that take hours to run and model fractured explicitly are compared with other more computationally efficient modelling approaches
- In order to provide accurate results while modelling fractured in 2ft wide blocks, the flow is "pseudo-ized" by applying a non-Darcy correction factor to the Forcheimer number in blocks that represent fractures.

Conclusions Reached:

- Standard dual permeability modelling cannot accurately model flow in very low permeability shales
- When used in conjunction with a Forcheimer correction factor, the LS-LR-DK model can produce results that are consistent with much more computationally expensive high resolution models
- The same model can also be used to accurately model flow in stress sensitive fractured shale reservoirs

Comments:

- Examines 2D flow only
- Dry gas simulations

SPE 160099 (2012)

Phase Behaviour of Gas Condensates in Shales Due to Pore Proximity Effects: Implications for Transport, Reserves and Well Productivity

Authors: D. Devegowda, K. Sapmanee, F. Civan, R. Sigal

Contribution:

- A quantitative approach describing the underlying physical phenomena that is unique to nanoporous shales, and critical in understanding field production and well performance in these systems.

Objective:

- To quantify the impact of pore wall geometry on gas condensate properties
- To investigate in particular the real gas behaviour and phase behaviour under pore proximity adjusted critical conditions

Methodology Used:

- Conventional reservoir simulation adapted to include the modifications of critical parameters as a result of pore geometry effects

Conclusions Reached:

- Nano pores seem to be beneficial in the productivity of liquids rich shale systems due to the reduction of condensate dropout caused by pore geometry effects
- The approach given in this work can be applied for use in existing compositional simulators, without requiring access to the code of the simulator
- Pore proximity effects have a significant impact and an understanding of them is important for routine engineering calculations such as reserves, estimating the productive life of a well, and the productivity index

Comments:

- Technique can only be applied to a single porosity model

SPE 136873 (2010)

Evaluation of Stimulation Techniques Using Microseismic Mapping in the Eagle Ford Shale

Authors: A. Inamdar, R. Malpani, K. Atwood, K. Brook, A. Erwemi, T. Ogundare, D. Purcell

Contribution:

- Provides an overview of completions practices used in the Eagle Ford shale
- Investigates the use of the "relax-a-frac" technique with the use of microseismic mapping

Objective:

- To aid in the optimization of stimulation design by integrating engineering and reservoir parameters with microseismic mapping techniques

Methodology Used:

- Microseismic mapping

Conclusions Reached:

- The size of the ESV is strongly linked with production
- The relax-a-frac technique increases microseismic activity and ESV size
- Height growth is predominantly controlled by geological factors

SPE 152533 (2012)

Understanding Hydraulic Fracture Stimulated Horizontal Eagle Ford Completions

Authors: R. Shelley, L. Saugier, W. Al-Tailji, N. Guliyev, K. Shah

Contribution:

- Presents the results of a modelling study on the completion of hydraulically fractured wells in the Eagle Ford shale

Objective:

- To provide information that will enable better stimulation design through an enhanced knowledge of the relationships that are observed between design and production performance

Methodology Used:

- Data driven sensitivity study

Conclusions Reached:

- Gas production is strongly influenced by depth
- Gamma ray count related to oil and gas productivity
- The oil window of the Eagle ford requires different stimulation to the gas window – closer fracture spacing and the use of cross linked frac treatments are beneficial

SPE 147596 (2011)

Shale Oil Production Performance from a Stimulated Reservoir Volume

Authors: A.S. Chaudhary, C. Ehlig-Economides, R. Wattenbarger

Contribution:

- Investigates the production behaviour of shale oil from a stimulated reservoir volume
- Varies reservoir parameters to investigate their effect on recovery patterns

Objective:

- To evaluate the recovery potential for shale oil produced from above and below the bubble point pressure from very low permeability shale systems
- To investigate optimal gridding approaches to model shale oil systems

Methodology Used:

- Numerical simulation
- Based on Eagle Ford properties

Conclusions Reached:

- Logarithmic refinement capture the flow behaviour of shale oil well
- Closer fracture spacing is correlatable with both rates and cumulative recovery
- There is a high production sensitivity to critical gas saturation, core studies would be useful in clarifying this property

CSUG/SPE 138145

Petrophysical Characterization of the Eagle Ford Shale in South Texas

Authors: J. Mullen

Contribution:

- Presents an overview of the petrophysical properties in the Eagle Ford shale
- Advises on completion approaches with reference to reservoir characterization

Objective:

- To aid in understanding the reservoir through the integration of data-acquisition and reservoir characterization techniques

Methodology Used:

- Data acquisition and analysis
- Geological modelling

Conclusions Reached:

- The Eagle Ford varies significantly in petrophysical properties across the play. It is therefore not possible to generalise over any large area
- The shale-log petrophysical model integrates all available data from multiple sources, and can be used for decision making in development planning and completion design

CSUG/SPE 148751

An Integrated Approach for Understanding Oil and Gas Reserves Potential in Eagle Ford Shale Formation

Authors: L. Fan, R. Martin, J. Thompson, K. Atwood, J. Robinson, G. Lindsay

Contribution:

- Proposes a methodology to help operators describe the reserves potential and distribution in the Eagle Ford shale

Objective:

- To help foster an understanding of the distribution and potential of reserves in the Eagle Ford shale through the use of specialised integrated analysis

Methodology Used:

- Log analysis
- Production data gathering
- Geological analysis

Conclusions Reached:

- Eagle Ford production correlates with the overlying Austin Chalk production
- The strongest producers are found in the thickest regions of the Eagle Ford
- Completion design should consider the geological conditions, not necessarily a one-size-fits all approach due to the variation in the Eagle Ford

SPE 1600076

Production Analysis in the Eagle Ford Shale – Best Practices for Diagnostic Interpretations, Analysis, and Modelling

Authors: D. Ilk N. J. Broussard, T. A. Blasingame

Contribution:

- Presents diagnostic interpretations of 9 wells from different reions of the Eagle Ford shale along with an analysis of the trends and variations observed

Objective:

- To develop a methodology that aids in the effective analysis and modelling of the Eagle Ford Shale

Methodology Used:

- Numerical Modelling
- Diagnostic interpretation

Conclusions Reached:

- Diagnostic interpretation is important in understanding the behaviour of a producing well. They should be performed prior to efforts to model producing wells
- Differences in estimated ultimate recovery (EUR) trends observed from well to well are mostly due to the well completion, but may also be a result of variations in fluid properties